



**Maurício Neves
Rodrigues da Silva
Pereira**

Sensor Óptico “Usável”

Wearable Optical Sensor



**Maurício Neves
Rodrigues da Silva
Pereira**

Wearable Optical Sensor

Dissertação apresentada à Universidade de Aveiro para cumprimento dos requisitos necessários à obtenção do grau de Mestre em Engenharia Electrónica e de Telecomunicações, realizada sob a orientação científica do Dr. António Luís Jesus Teixeira, Professor Auxiliar do Departamento de Electrónica, Telecomunicações e Informática da Universidade de Aveiro

To my family who always stands beside me and is not always duly appreciated...

The jury

President

Prof. Dr. Paulo Miguel Nepumoceno Pereira Monteiro
Associate Professor of Universidade de Aveiro

Dr. Daniel Diogo Ferrão da Trindade Fonseca
NSN – Nokia Siemens Networks

Prof. Dr. António Luís de Jesus Teixeira
Associate Professor of Universidade de Aveiro

Prof. Dr. Rogério Nogueira
Researcher at Instituto de Telecomunicações

Acknowledgements

First of all I would like to express my gratitude for Dr António Teixeira for having accepted me in this work.

I'm also grateful to Lúcia Bairo for all the patience and help given during this long year.

I would like to thank to all my friends who, with simple and small gestures, helped me through all the rough times.

And last but not least, I would like to thank my parents, to my sister and Manuela for all their loving support, care, patience and wisdom.

palavras-chave

Fibra Óptica Plástico, Sensor Óptico de Flexão, Bluetooth, Acoplador, OpenGL.

resumo

Neste trabalho foi desenvolvido um sensor para medição do ângulo de flexão do cotovelo de um indivíduo. Este sensor é uma ajuda na aferição da recuperação de uma pessoa que sofreu um acidente cardiovascular e que tenha perdido mobilidade no conjunto ombro-braço. Embora o sensor por si só não desempenhe uma função vital na recuperação de um paciente com as características referidas, espera-se que se torne uma ajuda na motivação da pessoa bem como uma maneira de quantificar o desenvolvimento por parte do profissional de saúde.

Para este efeito, foi usada uma fibra óptica de plástico uma vez que reúne algumas características importantes para o trabalho a realizar, como é o caso do seu reduzido tamanho, peso e custo de produção, a sensibilidade a flexões macroscópicas e, devido ao diâmetro consideravelmente largo, facilidade em ser manuseada. Foram ainda investigados alguns métodos para tornar a referida fibra verdadeiramente sensível sendo também apresentados os resultados obtidos. Com o intuito de inovar, foi apresentado um novo método para a realização desta medição sendo o seu comportamento comparado com os procedimentos anteriores.

No âmbito desta dissertação, o sensor foi também integrado num sistema inteligente que permite o envio dos valores obtidos para um computador, sendo possível posteriormente a sua representação numa aplicação gráfica para uma melhor visualização. Este sistema possui um módulo de comunicações sem fios que visa aumentar a liberdade de movimentos do utilizador durante a execução do teste bem como diminuir ao máximo o incómodo causado pelo sensor.

keywords

Polymer Optical Fiber, Bend Optical Sensor, Bluetooth, Coupler, OpenGL

abstract

In this work a sensor to measure the bending angle of the elbow of an individual was developed. This sensor is a helping tool to ascertain the degree of recovery of a person who suffered a cerebral vascular accident resulting in a loss of mobility of the shoulder-arm set. Although the sensor itself plays no vital role in recovery of a patient with the mentioned damages it is expected that it will become a mean of motivation of the patient and also a way of measuring the progress by the health professional.

For this purpose a polymer optical fibre was used because it gathers some important features for the aim of this work such as being small and of little weight and not costly to develop, sensitive to macroscopic bendings and, due to its considerably large diameter, of easy handling. One has also investigated some methods to make the mentioned fibre truly sensitive to bending and the achieved results are also displayed. With the view to innovate a new method to perform this measurement is introduced and its behaviour compared to the previous procedures.

Within the frame of this thesis, the sensor has also been integrated in a smart system that allows capture and transmission of the achieved results to a computer to enable their posterior graphical representation for a better vision. This system has a unit of wireless communication aiming the increase freedom of movement of the user during tests and also to reduce as far as possible the discomfort caused by wearing the sensor.

Contents

Table of Figures.....	3
List of Tables.....	5
List of Acronyms.....	6
1. Introduction.....	7
1.1- Thesis structure.....	7
1.2- Motivation.....	8
1.3- Goals.....	9
1.4- Contributions.....	9
2. Basics of Fibre Optics.....	10
2.1- Snell's Law.....	10
2.2- Numerical Aperture.....	11
2.3- Optical Attenuation.....	12
2.4- Macro Bending Losses.....	13
2.5- Optical Couplers.....	15
3. Optical Sensing for Macro Bending.....	18
3.1- Introduction.....	18
3.2- Bend Sensing Using Long Period Fibre Gratings.....	18
3.3- Chemical Tapering.....	21
3.4- Radial Grooving.....	24
3.5- Side Polishing.....	28
3.6- Concluding Remarks.....	30
4. Implementation.....	32
4.1- Introduction.....	32
4.2- Sensor.....	32
4.3- Control Board.....	36
4.4- Graphical Application.....	39
4.5- Concluding Remarks.....	40
5. Results.....	42
5.1- Introduction.....	42

5.2- Sensor.....	42
5.3- Control Board	48
5.4- Graphical Application.....	50
5.5- Concluding Remarks.....	51
6. Conclusions	53
7. Future Work	54
8. References	55

Table of Figures

Figure 2.1.1- Schematic representation of Snell's Law.....	10
Figure 2.2.1- Representation of maximum acceptance angle (from [1]).....	11
Figure 2.4.1- Propagation in a bended fibre	13
Figure 2.4.2- Numerical Aperture influence in bending losses (from [2]).....	14
Figure 2.4.3- Influence of core diameter in bending losses (from [2])	14
Figure 2.5.1- Coupler schematic	15
Figure 2.5.2- 100% of power going to port 2 of the coupler.....	16
Figure 2.5.3- 100% of power going to port 3 of the coupler.....	16
Figure 2.5.4- Power equally distributed by ports 2 and 3 of the coupler	16
Figure 2.5.5- Same coupling region length using two different wavelengths (1,3 μm and 1,55 μm , respectively)	17
Figure 3.2.1- LPG fabrication using an UV laser.....	19
Figure 3.2.2- Evolution of LPG attenuation band centre wavelength against curvature for $\theta=0^\circ$ and 180° , where θ is the rotational angle of the fibre (from [6]).....	20
Figure 3.2.3- Transmission spectrum of an attenuation band in the spectrum of a LPG experiencing different bend curvatures. Solid Curve, curvature 0.00 m^{-1} ; dashed curve, curvature 1.55 m^{-1}	20
Figure 3.3.1- Schematic of a typical fibre taper	21
Figure 3.4.1- Schematic of the optical flow sensor in one dimension (from [8]).....	24
Figure 3.4.2- Front and top views of a section of the fibre optic flowsensor used to measure the two-dimensional fluid flow (from [8]).....	24
Figure 3.4.3- Parameters of the "imperfected" area (from [9]).....	26
Figure 3.4.4- The transfer functions for changes in abrasion angle ψ (a), imperfection location γ (b), imperfection location l (c) and V-groove depth d (d) (from [9]).	26
Figure 3.5.1- Side Polished Fibre in straight position and in convex and concave bending (from [10]).	28
Figure 3.5.2- Power attenuation due to bending flexion angle with Red and Green Led (75% of the initial diameter polished with 15 mm of length) (from [14]).....	28
Figure 3.5.3-Three cycles bending/extension of a 50% side-polished fibre with $l=17$ and 40mm and red LED as light source (from [14]).....	29
Figure 3.5.4- All polished fibres with free bending length of 15mm and red LED as light source (from [14]).....	29
Figure 4.2.1 –Sensor made with two side-polished fibres in straight position and with fibre 1 suffering a convex and concave bending.....	33
Figure 4.2.2- LED polarization circuit schematic	34
Figure 4.2.3- Photo-detector circuit schematic.....	34
Figure 4.2.4- Amplification circuit schematic.....	35
Figure 4.3.1- Control Board photograph	36
Figure 4.3.2- Bluetooth module photograph	37
Figure 4.3.3- Protection circuit schematic.....	38
Figure 5.2.1- Arm simulator photograph.....	42

Figure 5.2.2- Voltage vs Angle with a single POF.....	43
Figure 5.2.3- Results obtained with different techniques of increasing sensibility in POF	43
Figure 5.2.4- Power attenuation due to bending angle on three different couplers (coupler1 with 1.4 cm of polished area length; coupler 2 with 1.0 cm of polished area length; coupler 3 with 2.0 cm of polished area length)	44
Figure 5.2.5- Light emitter, receiver and amplification circuit photograph.....	45
Figure 5.2.6- Photograph of the sensor applied on the sleeve.....	46
Figure 5.2.7- Photograph of the sensor correctly applied in the arm	46
Figure 5.2.8- Voltage vs bending flexion angle with the sensor applied in a real arm (3 cycles bending/extension with black lines representing bending process and grey lines showing extension process).....	47
Figure 5.3.1- MAX232 circuit schematic.....	48
Figure 5.3.2- Hyperterminal showing values sent by the PIC.....	49
Figure 5.3.3- Hyperterminal showing the direct result of the ADC conversion	49
Figure 5.4.1- Graphical Application environment	51
Figure 5.4.2- Output text file of the graphical application	51

List of Tables

Table 1.2.1- Causes of Stroke.....	8
Table 3.2.1- Advantages and disadvantages in performing bend sensing with LPGs.....	21
Table 3.3.1- Advantages and disadvantages in chemical tapering.....	23
Table 3.4.1- Advantages and disadvantages of using radial grooving for bend sensing.....	27
Table 3.5.1- Advantages and disadvantages of using side polishing for bend sensing.....	30

List of Acronyms

CVA	Cerebrovascular Accident
POF	Polymer Optical Fibre
NA	Numerical Aperture
LPG	Long Period Grating
LED	Light Emitting Diode
PCB	Printed Circuit Board
PIC	Programmable Interrupt Controller

1. Introduction

1.1- Thesis structure

This thesis is divided into seven chapters as follows:

Chapter one describes the motivation of this work, the structure of the document followed by the goals on aimed at and, finally, the contributions of this thesis.

Chapter two focus on some basic optical concepts indispensable for the right understanding of the rest of the thesis.

Chapter three gives a thorough description of some methods used to perform bend sensing, reveals some of the results obtained in some reference papers and points out the main advantages and disadvantages of each procedure. Some conclusive notes drawn on these methods are exposed in the final part of this chapter.

Chapter four presents the full scheme of the structure designed to perform the bend sensing in a person's elbow, with full explanation of the reasons for all choices made.

Chapter five shows some of the most important results obtained along this thesis and the main conclusions one could draw from the results that were achieved.

Chapter six presents some concluding remarks about the whole of the thesis.

Chapter seven ends this thesis by presenting some comments about the future work that can be done to improve the created *Wearable Optical Sensor*.

1.2- Motivation

A stroke, also known as cerebrovascular accident or CVA, is the sudden death of brain cells due to a problem with the blood supply. When blood flow to the brain is impaired, oxygen and important nutrients cannot be delivered. The result is abnormal brain function. Blood flow to the brain can be interrupted by either a blockage or rupture of an artery to the brain. There are many causes for a stroke, as shown in the table 1.2.1.

Causes of Stroke	
Blockage of an artery	Clogging of arteries within the brain (for example, lacunar stroke) Hardening of the arteries leading to the brain (for example, carotid artery occlusion) Embolism to the brain from the heart or an artery
Rupture of an artery (hemorrhage)	Cerebral hemorrhage (bleeding within the brain substance) Subarachnoid hemorrhage (bleeding between the brain and the inside of the skull)

Table 1.2.1- Causes of Stroke

A stroke is one of the main causes of death in several countries in the world and is a leading cause of physical and mental incapacitation. Stroke can affect people in different ways. It depends on the type of stroke, the injured area of the brain and the extent of the brain damage. Brain injury from a stroke can affect the senses (such as eyesight, touch, awareness of body position, motor activity (movement of arms or legs), speech and the ability to understand speech. It can also affect behavioural and thought patterns, memory and emotion. Paralysis or weakness (the inability to move the arms or legs properly or at all) on one side of the body is also common. After a stroke, most of these problems can improve over time but in some patients they will go away completely. Although most gains in a person's ability to function in the first 30 days after a stroke are due to spontaneous recovery, rehabilitation has an important role. For the most part, successful rehabilitation depends greatly on several factors such as how early rehabilitation begins, the extent of the brain injury, the survivor's attitude, the cooperation of family and friends and the rehabilitation team's skill.

In fact, both rehabilitation and patient's mental attitude are vital factors in a recovery. The acknowledgment of this fact brought up the need to create a system to evaluate a patient's recovery, specifically, the recovery of the mobility in one or both arms. This structure is

important for both patient motivation and for results quantification by the rehabilitation team.

Despite aiming at patients who suffered a CVA, the designed device can be applied in all processes of rehabilitation independent from the disabling cause.

1.3- Goals

The main goal is to develop a small device possible to be used without causing any discomfort and capable of measure the bend of a human body articulation, more precisely the elbow articulation.

This device must be based upon an optical technology and must connect wirelessly with a PC where the results are shown in a 3D visualization. Data saving is also an imperative and power saving a concern.

1.4- Contributions

The main contributions of this work were:

1. Implementation of a sensor capable of performing bend sensing in a human's arm using a variable POF coupler.
2. Comparison between the results obtained with this new method and the results achieved with the most used techniques.
3. Integration of the sensor in a smart structure capable of receiving data from the sensor and send it off to a computer or other device using Bluetooth technology
4. Creation of graphical application for data representation and saving in a computer.
5. Publication: Maurício S. Pereira, António L. J. Teixeira, Rogério Nogueira, "Wearable Optical Sensor", SEON 2008 – VI Symposium on Enabling Optical Networks and Sensors, Porto, 20th June, 2008

2. Basics of Fibre Optics

2.1- Snell's Law

The first concept one need to understand in optical fibres is the concept of the refractive index (η) of one medium. It is a ratio between the velocity of light propagating in the vacuum (C_v) and the velocity of light propagating in a different medium (C_m). This ratio can be represented as:

$$\eta = \frac{C_v}{C_m} \quad (1)$$

An optical fibre is composed by two different mediums. The one inside is called the core and has refractive index of η_1 and the outside medium called cladding with refractive index of η_2 . When a ray of light travels through the first one, it reaches the boundary between the two mediums and a part of its energy is reflected with the same incident angle and the other part is refracted into the second medium. The refraction can be expressed by:

$$\frac{\sin\theta_1}{\sin\theta_2} = \frac{\eta_1}{\eta_2} \quad (2)$$

This expression is the well-known Snell's Law. One schematic representation of this law is shown in figure 2.1.1.

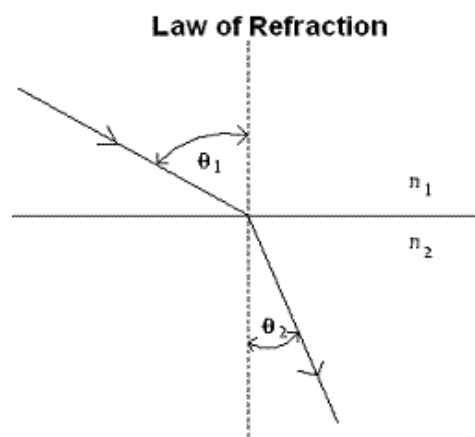


Figure 2.1.1- Schematic representation of Snell's Law

When the incident angle reaches a certain value, the refracted ray passes perpendicular to the normal ($\theta_2=90^\circ$). This incident angle is called critical angle (θ_c) and it is given by (3). Any incident angle beyond this value produces total internal reflection which means that no energy is transmitted to the second medium and all energy is reflected back into the first medium.

$$\theta_c = \sin^{-1} \frac{\eta_2}{\eta_1} \quad (3)$$

2.2- Numerical Aperture

Another important concept that one has to understand is the numerical aperture (NA) concept. In simple terms, there is a maximum angle from the fibre axis at which a ray of light may enter the fibre so that it will propagate in the core of the fibre. The sine of this angle is the numerical aperture of the fibre. A schematic representation of this concept is shown in figure 2.2.1.

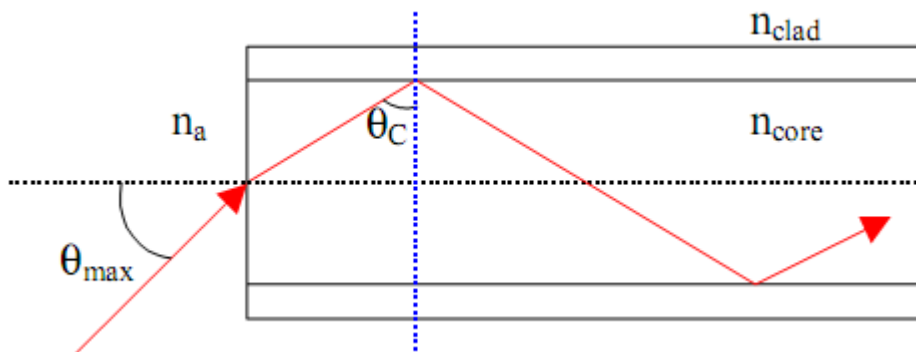


Figure 2.2.1- Representation of maximum acceptance angle (from [1]).

A possible approximation to obtain numerical aperture can be expressed by (4).

$$NA = \sin \theta_{max} = \sqrt{\eta_1^2 - \eta_2^2} \quad (4)$$

Fibre with large NA requires less precision to splice and work with than a fibre with a smaller NA. Usually, POFs have a larger NA when compared to glass fibres.

2.3- Optical Attenuation

Optical attenuation or power loss of an optical fibre is the loss of optical power as light rays propagate along a fibre and it is defined by the ratio between the optical power input (P_{in}) and the optical power output (P_{out}). Usually it is presented as a unit of length and given by the following expression:

$$attenuation = \frac{10}{L} \log_{10} \left(\frac{P_{in}}{P_{out}} \right) \quad (5)$$

Where L is the length of the fibre in kilometres and attenuation is expressed in dB/Km.

While a silica fibre can achieve attenuation values of 0.2 dB/Km, POFs currently available provide values of attenuation between 30 and 200 dB/Km and that is the main reason why only glass fibres are used for long distance communication.

There are three main types of attenuation in a fibre. They are absorption losses, scattering losses and bending losses. The first one is caused by the fibre itself or by impurities in the fibre such as water and metals. There are two types of absorption: intrinsic which is caused by interaction with one or more components of the glass and extrinsic, caused by impurities within the glass.

Regarding the second cause of attenuation, scattering loss, is an intrinsic loss mechanism caused by the interaction of photons with the glass itself. Again, it can be divided in two different kinds: Rayleigh scattering and Mie scattering. Rayleigh scattering takes place when the size of the defect (density fluctuation in the fibre) is less than about one-tenth of the wavelength of light being used. This is the dominant scattering mechanism in silica fibres. If the size of the defect is greater than one-tenth of the wavelength it is called Mie scattering.

Concerning the last source of power loss, bending, once again, it can be divided in two different groups: micro and macro bending. Micro bending losses are caused by irregularities in core-cladding interface and possible bendings inside the fibre with curvature radius much smaller than the wavelength being used. Macro bending losses are caused by curvatures in the fibre with curvature radius much larger than the wavelength of operation. This last cause of losses is the main principle of optical sensors because it is possible to establish a relation between the optical attenuation and the bending radius of the fibre.

2.4- Macro Bending Losses

Macro bending losses exist because, when a fibre is bended, the incident angle that a ray of light propagating in the fibre does with the normal to the interface core-cladding becomes smaller and smaller. As explained in section 2.1 of this thesis, if this angle becomes smaller than the critical angle total internal reflection no longer exists. This means that some part of the energy of the ray of light is refracted to the cladding and consequently produces losses. This effect grows as the angle of bend increases because fewer reflections are needed so that the incident angle becomes smaller than the critical angle. This phenomenon can be observed in figure 2.4.1.

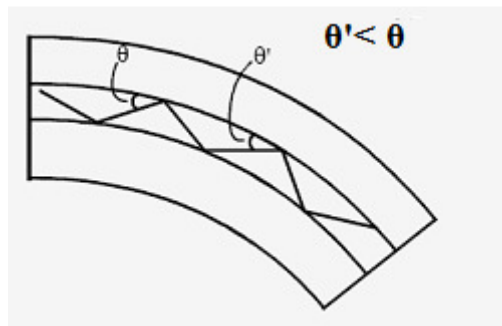


Figure 2.4.1- Propagation in a bended fibre

There are two main parameters that can influence the amount of losses that a fibre suffers during a bend, for a given bend radius [2]. Those parameters are the numerical aperture of the fibre and its core diameter.

As seen in section 2.2, numerical aperture of a fibre is given by the expression (4). It is trivial to see that the value of NA can be related with both core and cladding refractive indexes. If one compares this expression to formula (3) from section 2.1 that establishes a relation between the critical angle and the ratio $\frac{\eta_2}{\eta_1}$ it is possible to understand that, if NA is increased, the referred ratio decreases and the critical angle value will also decrease. Therefore, there are more angles that are likely to cause total internal reflection and will make the angle variation provoked by bending less damaging. This effect is shown on figure 2.4.2.

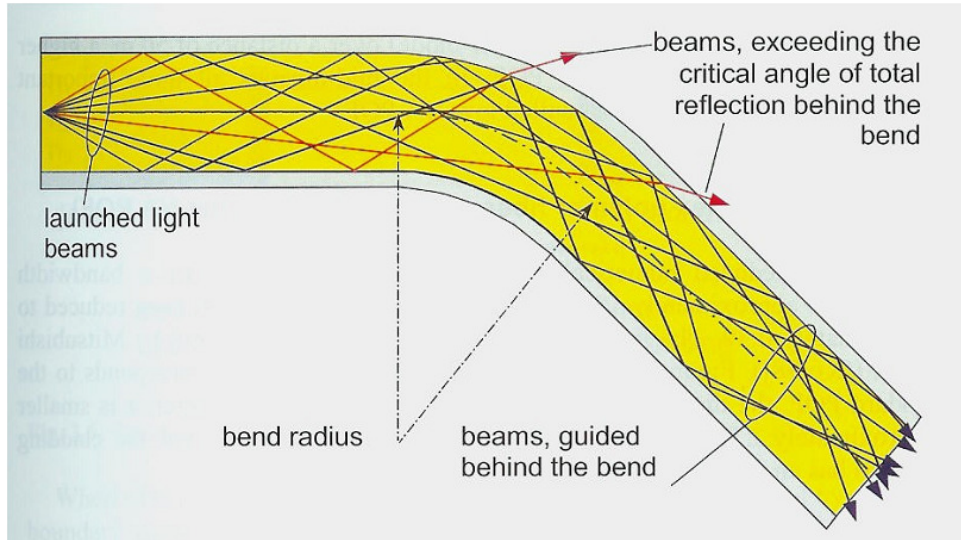


Figure 2.4.2- Numerical Aperture influence in bending losses (from [2]).

As for the second parameter, the core diameter, it is possible to establish a relation between this measure and bending losses. When the core radius decreases, the number of modes travelling through the fibre also decreases as well as the power fraction in the cladding. Some graphics showing these results can be seen in figure 2.4.3.

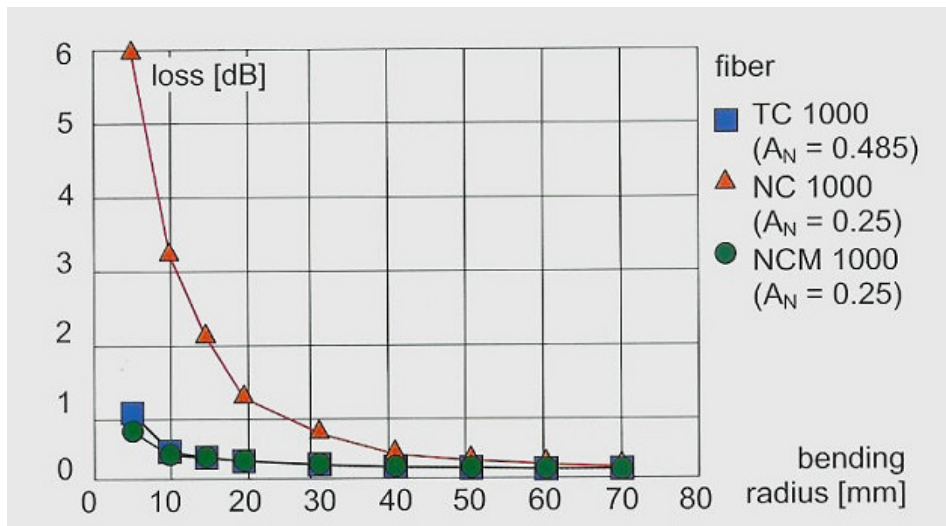


Figure 2.4.3- Influence of core diameter in bending losses (from [2])

2.5- Optical Couplers

A fibre coupler is an optical fibre device with one or more input fibres and one or several output fibres where light from an input fibre can appear at one or more outputs. The power distribution among the outputs depends on the wavelength and coupling length. There are several different fabrication processes to manufacture a coupler:

- Fibers can be thermally tapered and fused so that their cores come into close contact.
- Some couplers use side-polished fibres, providing access to the fibre core.
- Couplers can also be made from bulk optics, for example, in the form of micro lenses and beam splitters, which can be coupled to fibres (“fibre pig-tailed”).

Fibre couplers are usually directional couplers which means that essentially no optical power sent into some input port can return into one of the input ports. To indicate how weaker the back-reflected light is when compared with the input, there is often a specification of *return loss*. One schematic of a coupler with two input and two output ports can be seen in figure 2.5.1.

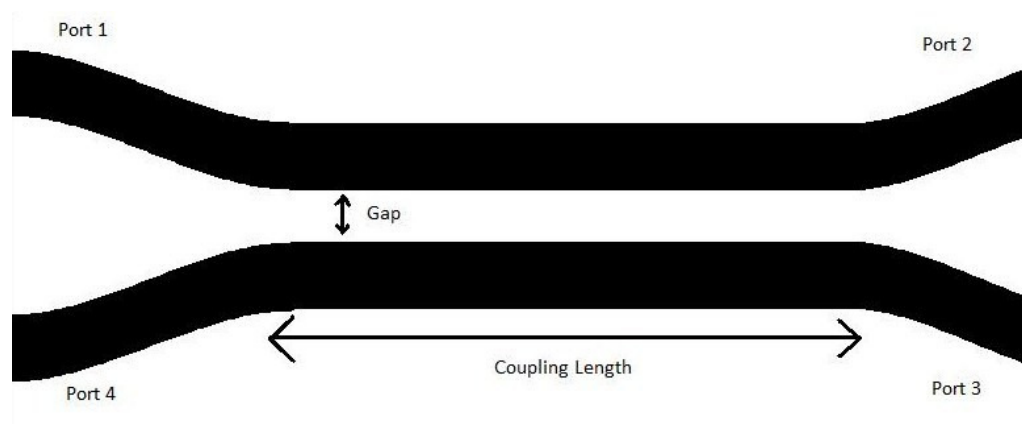


Figure 2.5.1- Coupler schematic

In order to explain the mode of operation of the shown coupler it will be considered that light enters on port 1 and that, for a given wavelength, the coupling length is the length needed to transfer 100% of power from one given input port to the other fibre. As light propagates, optical power will be transferred to the inferior core. If the coupling length is long enough, there will be another power transfer to the previous core. This process will repeat until the coupling region ends. Depending on the coupling section length, there can be different instances for the power profile at the end of the coupler. For example, 100% of the power can appear in port 2 (case shown on figure 2.5.2) or, if the coupling length is

reduced to a half, all power can emerge on port 3 (figure 2.5.3) or, if the referred length is one fourth of the original value, power can be divided for both ports 2 and 3 in equal quantities, as one can see in figure 2.5.4.

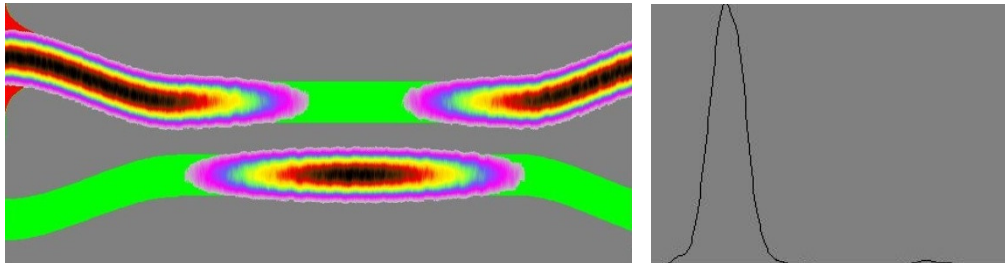


Figure 2.5.2- 100% of power going to port 2 of the coupler

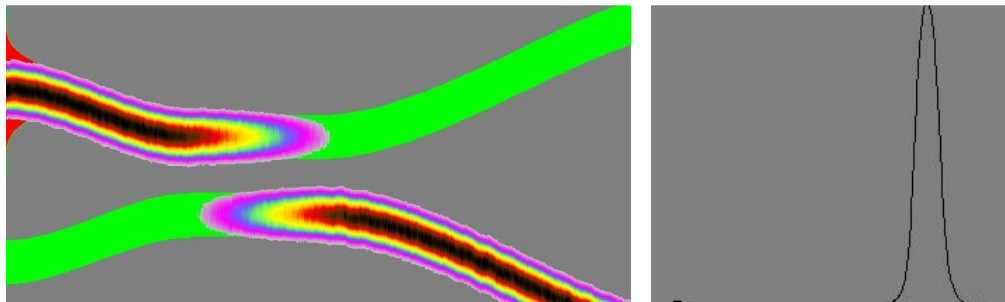


Figure 2.5.3- 100% of power going to port 3 of the coupler

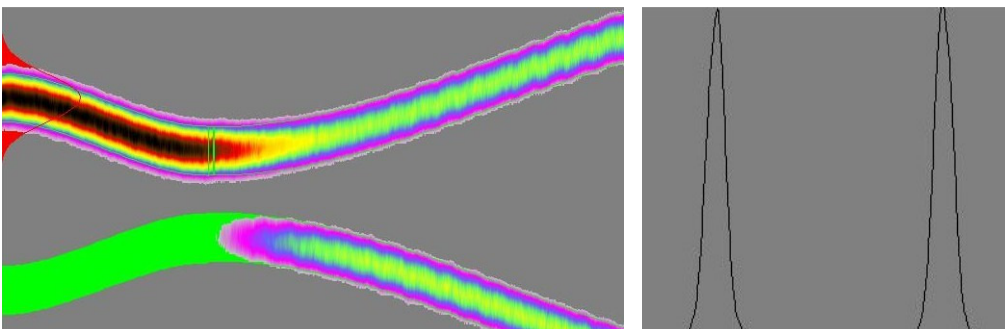


Figure 2.5.4- Power equally distributed by ports 2 and 3 of the coupler

On the right side of all three figures, one can see the power profile at the end point of the coupler. As one can see on figure 2.5.2, almost all the power went to port 2 and, of course, none for port 3. In the opposite case and as figure 2.5.3 shows, when the coupling region is reduced to half of its original value, all the power introduced into the coupler goes to port 3. In the last case, the power is divided almost equally to both to ports 2 and 3. This situation

happens when the coupling region length is half of the precedent situation or one fourth of the initial value. Couplers with this last configuration are usually called *3 dB couplers*.

However, the length of the coupling region is not always the same. It essentially depends on two factors: the size of the gap between both cores (the further away both cores are from each other, the greater will be the coupling region length) and the wavelength of the propagating wave (different wavelengths lead to different coupling regions). The effect produced by the last cause can be seen in the following figure.

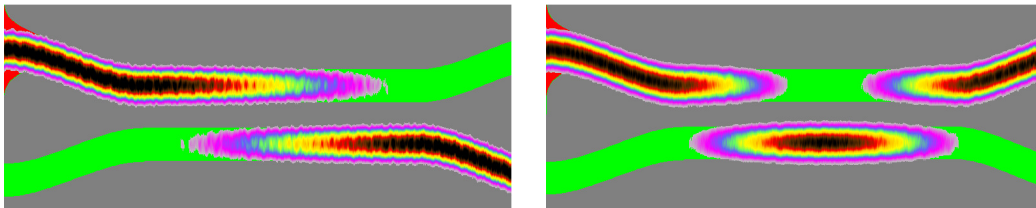


Figure 2.5.5- Same coupling region length using two different wavelengths (1,3 μm and 1,55 μm , respectively)

All figures shown in this section were produced using a freeware software available on [15].

3. Optical Sensing for Macro Bending

3.1- Introduction

Over the last few years, the use of sensors based in optical fibres has been widely developed. In fields like civil engineering, industry, automobile fields, medicine or even home appliances, these sensors are being more and more introduced because of their advantages like their light weight, flexibility, low cost of production and electromagnetic immunity in relation to other technologies. This technology permits the measurement of a variety of attributes like pressure, strain, vibration, displacement, velocity, acceleration, temperature and humidity [3, 4].

On this thesis one will focus on the capability of a fibre to measure the macro bending, like the bend of an arm. There are several techniques to use optical fibres as sensors for bending and this chapter one will present some of them as well as their major advantages and disadvantages.

3.2- Bend Sensing Using Long Period Fibre Gratings

Fibre grating consists of a periodic modification of the properties of an optical fibre, generally of the refractive index of the core. These perturbations have two general classifications: Short-period fibre gratings or fibre Bragg gratings (FBG) and long period gratings (LPG). The first ones have a sub-micron period and act to couple light from the forward propagating mode of the optical fibre to a backward, counter propagating mode. This coupling occurs at a specific wavelength given by

$$\lambda = 2\eta_{eff}\Lambda$$

Where Λ is the grating period, λ is the vacuum wavelength and η_{eff} is the effective refractive index of light in the fibre. This causes the effect of a narrow band reflection filter. The Bragg wavelength is governed by the period of the FBG and the effective index of the propagating mode, with the result that a change in either of these parameters, induced for example by a change in temperature or strain, changes the wavelength, forming the basis of the many reported FBG sensing schemes.

The long-period grating (LPG) has a period typically in the range of 100 μm to 1 mm. Such gratings couple the fundamental mode with the cladding modes of the fibre, propagating in the same direction. The high attenuation of the cladding modes results in the transmission spectrum of the fibre containing a series of attenuation bands centred at discrete wavelengths, each attenuation band corresponding to the coupling to a different cladding mode. The exact form of the spectrum, and the centre wavelengths of the attenuation bands, are sensitive to the period of the LPG, the length of the LPG (typically of the order of 30 mm) and to the local environment: temperature, strain, bend radius and to the refractive index of the medium surrounding the fibre. Any change in these parameters produces a modification in the period of the LPG and in the difference between both core and cladding modes refractive indexes. This modification will change the phase matching conditions coupling to the cladding modes which results in a modification of the central wavelengths of the attenuation bands.

The most used process for LPG fabrication is achieved by ultraviolet irradiation [5], as it can be seen in Figure 3.2.1, but it can also be achievable by ion implantation, irradiation by femtosecond pulses in the infrared, irradiation by CO_2 lasers, diffusion of dopants into the core, relaxation of mechanical stress and electrical discharges. All these processes modify permanently the refractive index of the core of the optical fibre. But it is also possible to fabricate a LPG by physical deformation of the fibre which is achieved mechanically, by tapering the fibre or by deformation of the core or the cladding.

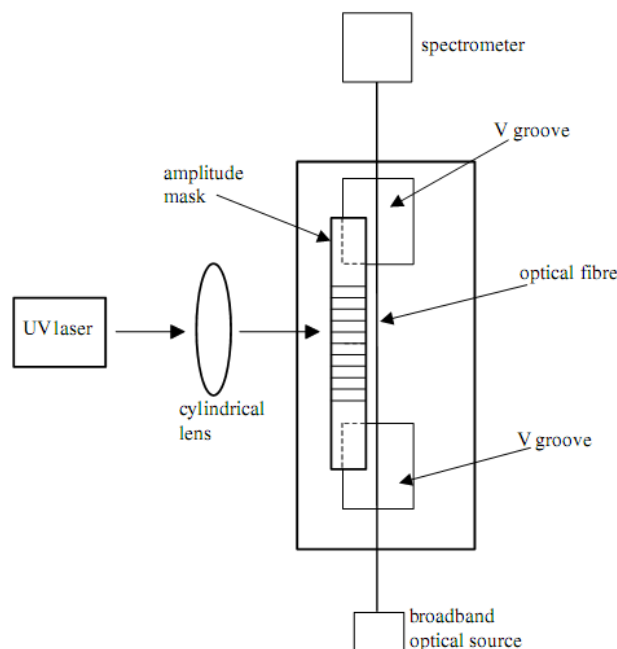


Figure 3.2.1- LPG fabrication using an UV laser

The bend sensibility of the LPG has two different forms of manifestation: it can produce a shift on the central wavelength of the attenuation band or cause a splitting in two of each attenuation band, with the wavelength separation of the split components increasing with increasing curvature. Some results showing these two phenomena can be seen in Figures 3.2.2 and 3.2.3.

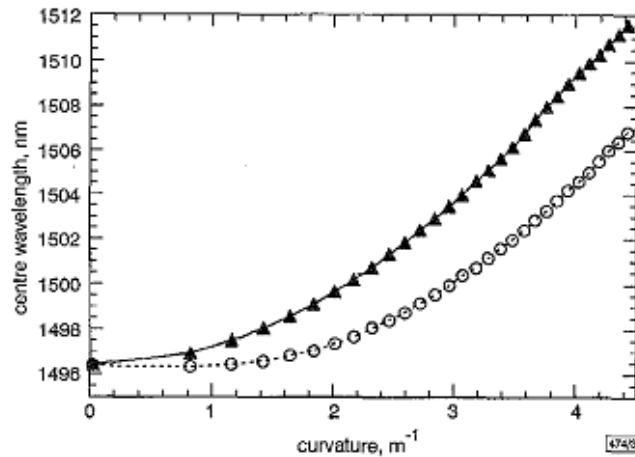


Figure 3.2.2- Evolution of LPG attenuation band centre wavelength against curvature for $\theta=0^\circ$ and 180° , where θ is the rotational angle of the fibre (from [6])

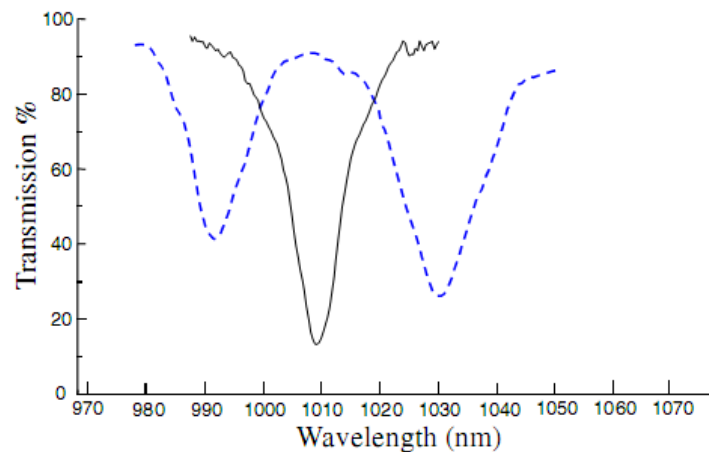


Figure 3.2.3- Transmission spectrum of an attenuation band in the spectrum of a LPG experiencing different bend curvatures. Solid Curve, curvature 0.00 m⁻¹; dashed curve, curvature 1.55 m⁻¹.

The presented method has some advantages and disadvantages summarized in the following table:

Advantages	Disadvantages
<ul style="list-style-type: none"> • Hability of measuring different attributes (strain, bend radius, temperature...) • High sensibility in bend sensing • Possibility of using two different manifestations to measure the same property 	<ul style="list-style-type: none"> • Complexity of fabrication process when compared to other methods

Table 3.2.1- Advantages and disadvantages in performing bend sensing with LPGs

The process of fabrication of a LPG is not simple to perform and that was the main reason why this procedure was not chosen to be within the frame of this thesis. Since for this work one was only interested in measuring bending and no other attributes, one would not take advantage of the main benefit of this method.

3.3- Chemical Tapering

A tapering consists in a localised diameter reduction of a fibre. A schematic of a fibre taper is shown on figure 3.3.1. This process can be done in several ways depending on the type of fibre that it is supposed to change. Although creating a taper in a silica optical fibre is a well-known process for many years, the same process in a polymer optical fibre was only introduced by D.F. Merchant *et al* [7] in 1999. The usual methods for tapering a silica based fibre are flame-drawing and acid etching.

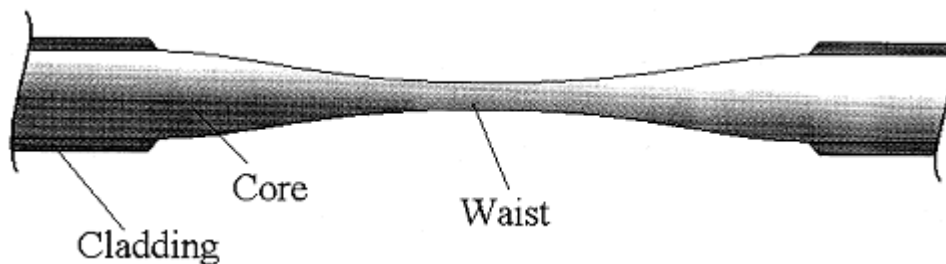


Figure 3.3.1- Schematic of a typical fibre taper

The first method consists in heating a section of the fibre with a clean gas flame or a laser source with temperatures close to the glass transition temperature and then pull the fibre before it cools down. This process cannot be done in a POF because the polymers used have low ductility and tendency for uneven melting which leads to breakages or total melting of the fibre.

The second process consists on etching the silica fibre with concentrated hydrofluoric acid. This process is unable to maintain the cladding intact and it requires handling with great caution due to the dangerous nature of the acid used. Like the first method, this one also cannot be used in POF directly because the solvent would dissolve all the polymers and would not cause just a surface effect.

What was proposed in the work referred above was a special mixture of solvents that could remove the cladding without destroying the core inside and then, with another mixture of solvents, proceed with the core tapering.

The first step is to remove the cladding. This is done by applying a few drops of 100% acetone in a tissue previously folded in two and allowed to hang on the fibre. Immediately after dropping the acetone in the tissue, this is rotated and caused to slide along the region one wants to treat. This procedure must be done with great care because the fibre becomes very fragile and can break if subject to any kind of pressure. After a period of 10 seconds of this movement, one has to apply in the tissue the same quantity of distilled water creating a mixture with the same quantity of acetone and water. Then, the cladding can be removed by gripping the tissue between the fingers and briskly rub it along the region treated. Finally, the core must be washed in water to restore the original physical and chemical properties of the core.

The second phase of this process is the tapering of the core. This is done by immersing the fibre in a solution specially prepared. This solution is composed by 60% acetone, 20% methyl isobutyl ketone (MIBK) and 20% distilled water. Depending on the final reduction required, the process can take from one hour to several days. By controlling the immersion time and the removal of the fibre, different taper profiles can be achieved. These profiles can vary from smooth variation of the diameter to step profiles.

Although this method can be used to create inline tapers and fibre end tapers, inline tapers are limited to a minimum of 2-3 cm due to the difficulty of immersing small lengths in a solvent bath. The creation of fibre end tapers can be as small as 1mm.

In order to summarize the advantages and drawbacks of this method, the following table is presented.

Advantages	Disadvantages
<ul style="list-style-type: none"> • Simple and low cost process • Requires no specialist equipment • Can produce a wide range of waist diameters and different taper profiles 	<ul style="list-style-type: none"> • Several hours needed to each a taper • Process involving acids although not highly concentrated • Requires a POF with a pure polymethylmethacrylate (PMMA) core and a doped Cytop cladding

Table 3.3.1- Advantages and disadvantages in chemical tapering

This method presents an organic solvent to perform tapering only in POFs with a very specific core and cladding components. The core must be made of a pure PMMA and the cladding with a doped Cytop cladding. Since available POFs are based in a different component of cladding this method could not be used in the context of this thesis.

3.4- Radial Grooving

The next method presented was proposed for the first time by R.Philip Candy *et al* [8] in 2000 within the attempt of developing an optical fibre drag-force flow sensor. This sensor was designed to measure the speed and direction of fluid flow. The schematic illustration of this sensor is showed in figures 3.4.1 and 3.4.2.

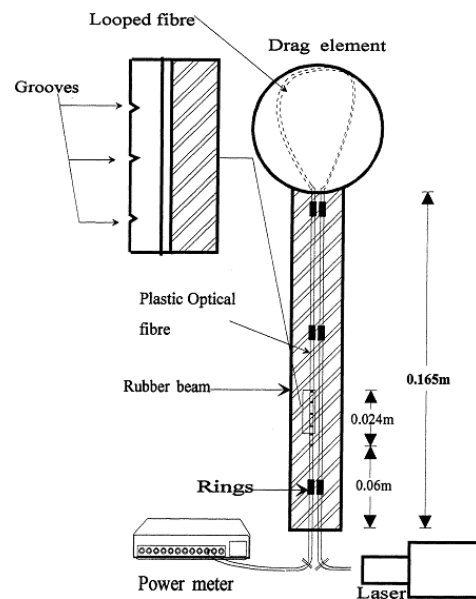


Figure 3.4.1- Schematic of the optical flow sensor in one dimension (from [8]).

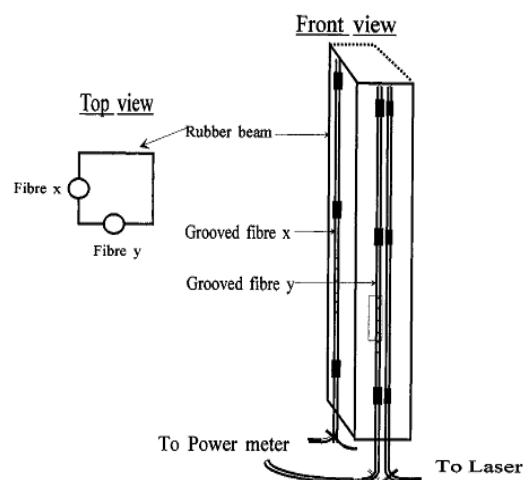


Figure 3.4.2- Front and top views of a section of the fibre optic flowsensor used to measure the two-dimensional fluid flow (from [8]).

As seen in the scheme, the sensor comprises a square cross-sectioned rubber cantilever which has a spherical drag element attached to its free end. The fibre used is a POF with 1mm diameter. The fibre was put along one face of the rubber beam and, to secure the fibre, plastic rings were attached to the same structure using epoxy. The rings were chosen carefully so that the fibre could slide along them freely without friction or snagging but small enough to ensure that the fibre followed the movement of the beam. The transmitting end of the fibre was connected to a laser but a Led could also be used for portability and the receiving end was connected to an optical power meter. In the fibre several grooves were made to maximize the sensor sensibility to bending. These grooves were located in the point where the maximum deflection of the fibre was achieved and were manufactured with the depth of 0.5 mm.

The principle of operation of this sensor is rather simple. As the cantilever bends in the presence of the airflow, the angles of the grooves varies. This effect produces a change in the light attenuation measured at the power meter that one can relate with the force inducing the bend, and therefore to the velocity of the fluid.

Within the scope of this thesis, the most important points of this method are the choice of the grooves location as well as their depth and number. As referred above, they were located in the point where the maximum deflection was exhibited in order to maximize the losses of the fibre during the bending process. For the same reason, the depth of the grooves has to be the maximum possible but without putting at risk the integrity of the fibre. If they were made too deep, the fibre probably would break in a short period of time due to the repetition of movements and the sensor would not achieve its purpose. As for the number of grooves made on the fibre, this would have to be a compromise between insertion losses and sensibility. If too many grooves are manufactured, the attenuation in the fibre even without bending will be very high and it will be more difficult to measure any variation. On the other hand, if the number of grooves is too low, the sensibility of the fibre to bending will be very low and variations will also be impossible to be detected.

A most complete study of the effect that grooves have in light attenuation during the bending process was proposed by A Babchenko and J Maryles [9] in 2006. On this work were studied the effect of several parameters on this process such as the groove cavity depth, the location of these imperfections and their orientation, as shown on figure 3.4.3.

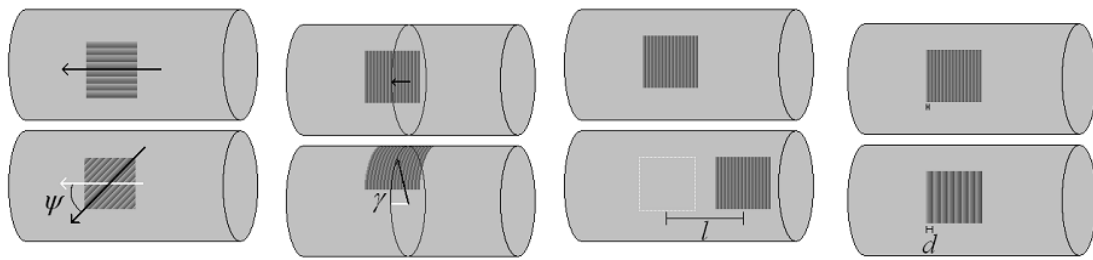


Figure 3.4.3- Parameters of the “imperfected” area (from [9]).

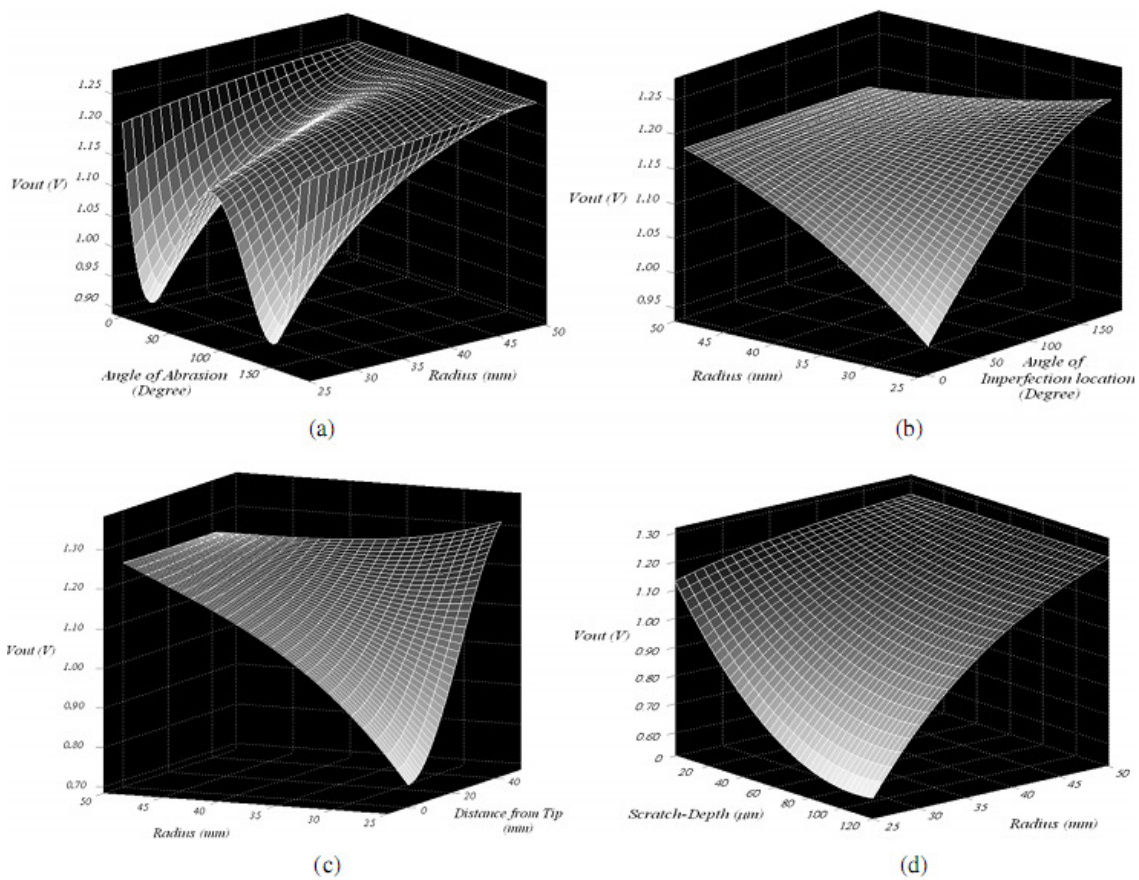


Figure 3.4.4- The transfer functions for changes in abrasion angle ψ (a), imperfection location γ (b), imperfection location l (c) and V-groove depth d (d) (from [9]).

Figure 3.4.4 shows the results achieved by the mentioned study. For all experiments, a single 5mm^2 was created and the fibre was bent over a radius range of 25-50 mm. As for the abrasion angle one can see that the sensibility of the sensor is very low when this angle is 0° (V-groove cavities parallel to the fibre axis). As the abrasion angle increases, the sensor becomes more sensitive because V-groove cavities open and more incident light escapes through the imperfected area. When the abrasion angle is near 90° , the sensibility of the sensor decreases because there is an increase in reverse reflection and double

refraction effects. Reverse reflection is when the light is reflected twice on the same side of the fibre in two different V-grooves. Double refraction happens when a ray of light is refracted out of the fibre and hits the opposite wall of the V-groove and is refracted back into the fibre.

As for the imperfection location angle γ , the maximal sensibility is achieved when this angle is 0° and 180° and, of course, at the angle of 90° the sensor's sensibility is almost zero. For the imperfection location, it can be seen that, as this value increases the sensibility of the sensor decreases as expected. In relation to the last parameter, V-groove depth, as this value increases the fibre becomes more sensitive to bending as a larger percentage of light travelling the fibre is affected by the imperfections.

Once more, to summarize all the advantages and drawbacks of the presented method, the following table is shown.

Advantages	Disadvantages
<ul style="list-style-type: none"> • Simple and low cost process • Requires no specialist equipment • Can be used in every type of POFs 	<ul style="list-style-type: none"> • If grooves depth is too deep, fibre integrity is compromised • Difficulty in controlling the precise depth of the grooving process which makes reproducibility somehow complex

Table 3.4.1- Advantages and disadvantages of using radial grooving for bend sensing

Due to its advantages, this was one of methods chosen to be tested in this thesis as one can see in section 5.2 of this document. Despite its disadvantages, this procedure is one of the most common approaches to perform bend sensing when using optical fibres. Since one of the main purposes of the author was to create a new technique to perform this measurement it was only tested and used for comparison but not used as final method.

3.5- Side Polishing

The next method that will be presented next was first introduced by Kuang *et al* [10] in 2002 and it is one of the most used techniques to sensitize a fibre [11-13]. This method uses the same principle of radial grooving. Some imperfections are created in the bent section of the optical fibre to increase the amount of radiation loss by this area. The difference between this method and the precedent one is that in this case the imperfections created are larger because they are made by side polishing some area of the fibre and can be as wide as several centimetres. An example of this operation can be seen on figure 3.5.1.

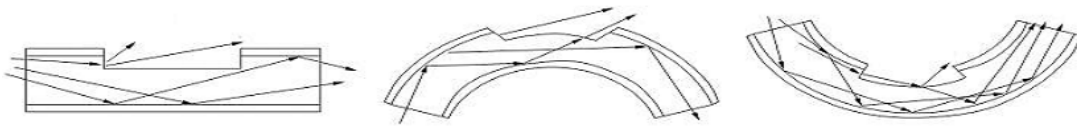


Figure 3.5.1- Side Polished Fibre in straight position and in convex and concave bending (from [10]).

Last year, a study was made by Bilro *et al* [14] about the impact of changing some parameters like the percentage of the diameter polished, the wavelength of light source and the polished length. For that an experimental set-up was implemented. It was constituted by a LED, a mechanical goniometer, a photo detector and a polymer optical fibre with 2.2 mm diameter including jacket.

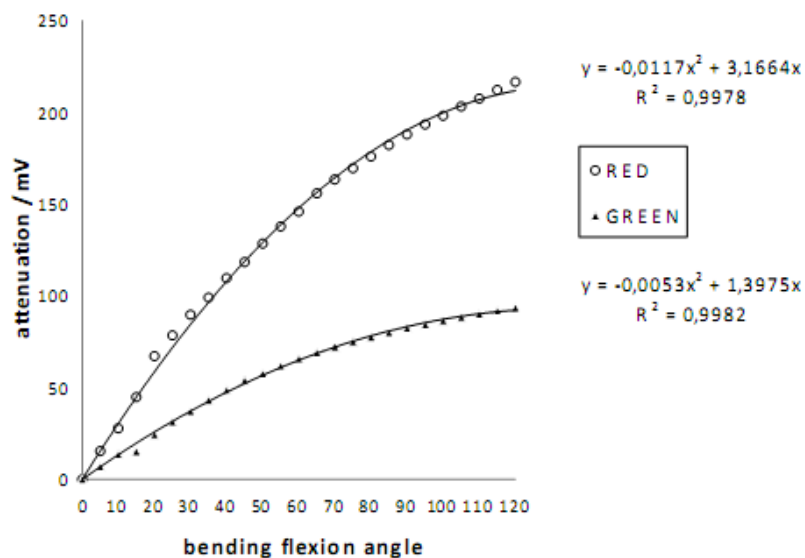


Figure 3.5.2- Power attenuation due to bending flexion angle with Red and Green Led (75% of the initial diameter polished with 15 mm of length) (from [14]).

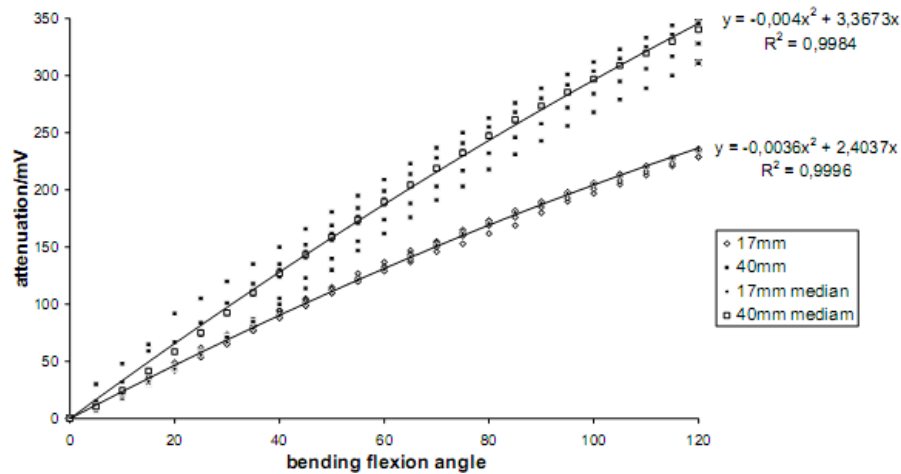


Figure 3.5.3- Three cycles bending/extension of a 50% side-polished fibre with $l=17$ and 40mm and red LED as light source (from [14]).

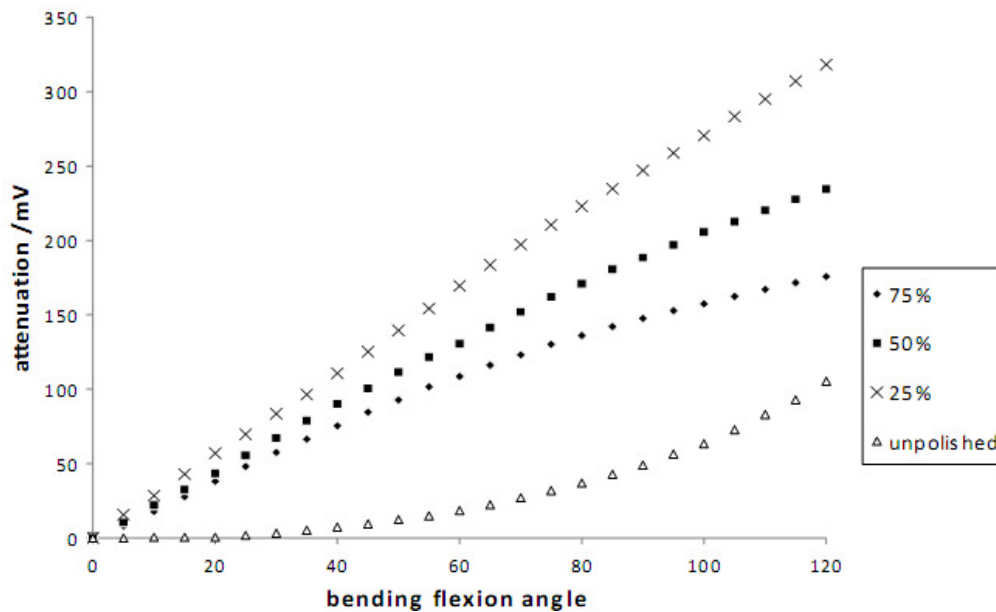


Figure 3.5.4- All polished fibres with free bending length of 15mm and red LED as light source (from [14]).

As one can see in figure 3.5.2, the red led has more sensibility than the green one. However, for this led, the polished length must be short to minimize hysteresis. In figure 3.5.3 one can see that, for polished length of 40 mm the hysteresis becomes not negligible. As for the polished depth, as can be seen on figure 3.5.4, the best sensitivity is achieved when only 25% of the initial diameter is polished. One important thing to retain is that the chosen fibre has approximately a linear behaviour during the bending process.

To summarize the advantages and disadvantages of the method presented in this section the following table is shown.

Advantages	Disadvantages
<ul style="list-style-type: none"> • Simple and low cost process • Requires no specialist equipment • Can be used in every types of POFs 	<ul style="list-style-type: none"> • If polishing depth is too deep, fibre integrity is compromised • Difficulty in controlling the precise depth of the polishing process which makes reproducibility somehow complex.

Table 3.5.1- Advantages and disadvantages of using side polishing for bend sensing

For the same reasons explained in the previous method, this method was tested but not used as the main method. This and the previous procedures have similar advantages and disadvantages because they are really similar to each other as their principle is to create imperfections on the fibre in order to increase losses when subjected to a flexion movement.

3.6- Concluding Remarks

In this chapter some methods to perform bend sensing were explained and their advantages and disadvantages were presented. These procedures are based on different principles to perform the referred measurement but follow a main course of action which is the creation of imperfections on the fibre in order to increase losses when bending.

Regarding the first method, the implementation of a LPG can be seen as the creation of an imperfection, a change of the refraction index, in a section of the fibre. The period of the interval this change is implemented will define the central wavelength the grating will reflect. During the bending process, due to the change of location of these imperfections, the reflected wavelength will also change thus enabling the possibility of using this method to perform the intended operation. This method also provides another manifestation when the fibre is suffering a bend. Instead of existing a central reflected wavelength, causing an attenuation band, due to the breaking of symmetry of the system another attenuation band is created and the separation between their central wavelengths separation dependent of the bend radius suffered.

As for the other methods, instead of creating imperfections just inside the core of the fibre, these are implemented in both the core and cladding. When a fibre is polished or a groove is done in the fibre, an imperfection is done in both the core and the cladding. When subject to a bending, light will escape through these flaws and this effect will increase as the bending degree grows. In a chemical tapered fibre, the reduction of its total diameter will result in a major reduction in the cladding. This will cause the core to be more exposed to external factors and, when experiencing a flexion, the evanescent field will rise and therefore increasing the fibre sensitivity.

4. Implementation

4.1- Introduction

In this chapter every part of the designed implementation of the wearable optical sensor will be shown and explained. This structure is responsible for creating the optical signal used to measure the bending angle of the arm, process this signal and send it to a computer. Once the information is on the computer, a graphical application will show the produced results in a 3D image and allow saving the results for other purposes.

4.2- Sensor

Despite some of the techniques presented on the precedent chapter of this work accomplish the objectives intended for this work, the intention of innovating somehow, led to the creation of another procedure that will be now introduced. This method is based on the one used by Bilro *et al* [14] but instead of using a single side-polished fibre, a variable coupler with two of these fibres was created. As explained in section 2.5 of this document, one of the possible procedures to fabricate a coupler is side polish a fibre to access its evanescent field.

The practical difference between this and the already existent method is that instead of measuring the amount of losses on fibre where light is inserted, one measure the amount of light coupled to the other fibre. The representation of the principle used in this sensor is shown on figure 4.2.1.

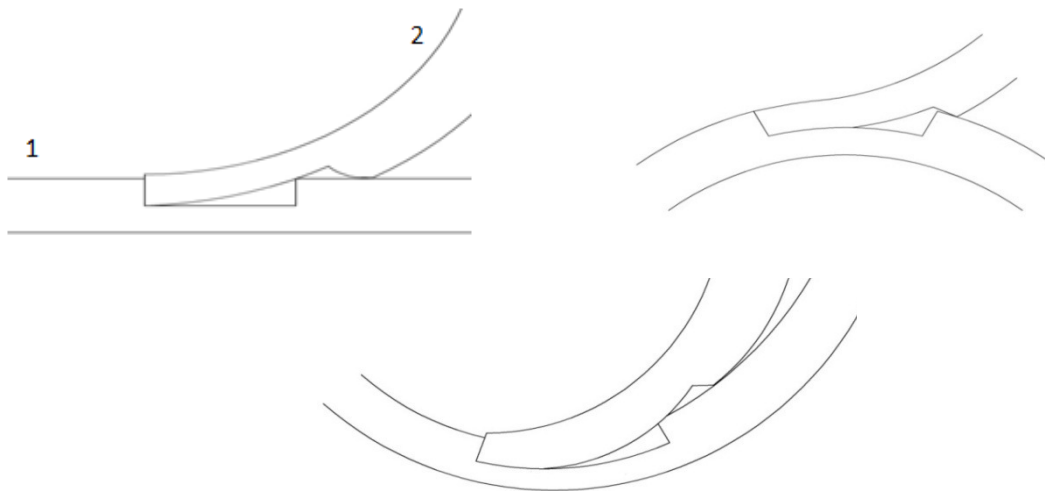


Figure 4.2.1 –Sensor made with two side-polished fibres in straight position and with fibre 1 suffering a convex and concave bending

On the fibre 2 end, a small drop of glue must be put in order to secure both fibres into each other. In addition to this, and to ensure that both fibre bend in the same axis, some duct tape was wrapped around both fibres uniting them. To improve the coupling effect a special gel was added in the coupling area. This gel is an index matching gel from Thorlabs (G608N). The function of this compound is to minimize reflections that are caused by the existence of air between both fibres creating a difference in both refractive indexes and, therefore, originating reflection losses.

If fibre 1 suffers a convex bending the evanescence field will increase as the polished area will grow. As the second fibre is glued to the first one, it accompanies this movement and the coupling will be greater. In the opposite situation, if fibre 1 suffers a concave flexion, the area polished will decrease so the evanescence field will also decrease. As expected this will produce a decrease in the amount of light coupled to fibre 2.

At the first end of fibre 1 is placed a green LED which is the optical source of this system. The LED chosen is an IF-E93 from Industrial Fibre Optics, Inc. This LED has wavelength of 530nm and is inserted in a special device that, despite its low cost, features an internal micro-lens to maximize optical coupling. For LED polarization a resistor was placed in series with the referred diode. This simple circuit is shown on figure 4.2.2.



Figure 4.2.2- LED polarization circuit schematic

At the free end of fibre 2 there must be a photo-detector to receive light and convert its optical power into electric current. For the same reasons that were explained above one has chosen the phototransistor IF-D92 also from Industrial Fibre Optics, Inc. Although this detector has its maximum sensibility at 870nm its behaviour for the used wavelength is good enough for this purpose. In order to use this detector a simple circuit was designed and can be seen in figure 4.2.3.

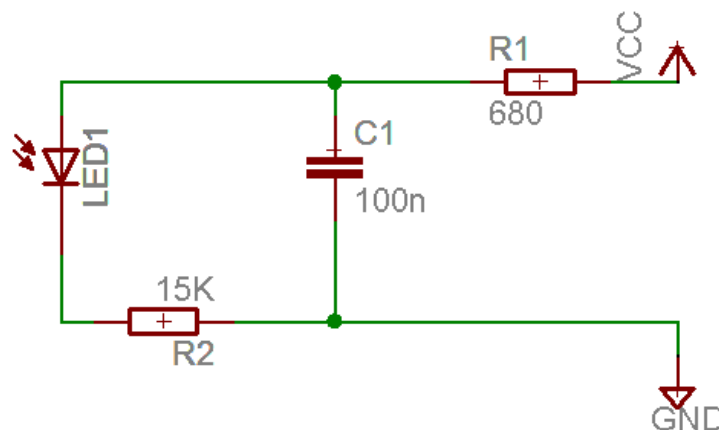


Figure 4.2.3- Photo-detector circuit schematic

As the sensor generates a signal with low voltage and in order to use the full scale of the ADC of the microcontroller, an amplifier was designed. This amplifier is essentially an OPAMP in its non-inverting configuration with a couple of resistors defining its gain. The chosen OPAMP was a MCP602 from Microchip. The choice was made according to several required characteristics such as being a rail-to-rail OPAMP and requiring a minimum voltage supply of 2.7V. The resistors used on the circuit depend on the sensor used. This circuit can be seen in figure 4.2.4.

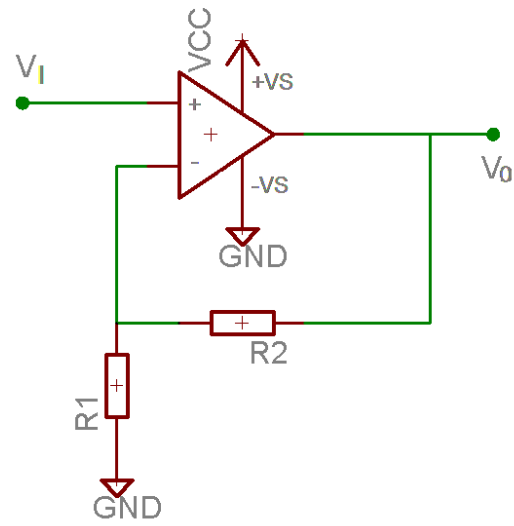


Figure 4.2.4- Amplification circuit schematic

4.3- Control Board

After having designed the sensor and having the signal ready to be processed, one needs to have a control board that allows data processing and transmission. This control board must be capable of doing a small processing of the signal into a format ready to be sent to a pc and must also be responsible for its transmission. A control board was already made by João Decoroso, for his final project and after an analysis of the referred board one concluded that it fulfilled all the requirements needed so it was chosen as the control board to be used. Its photograph can be seen on figure 4.3.1.

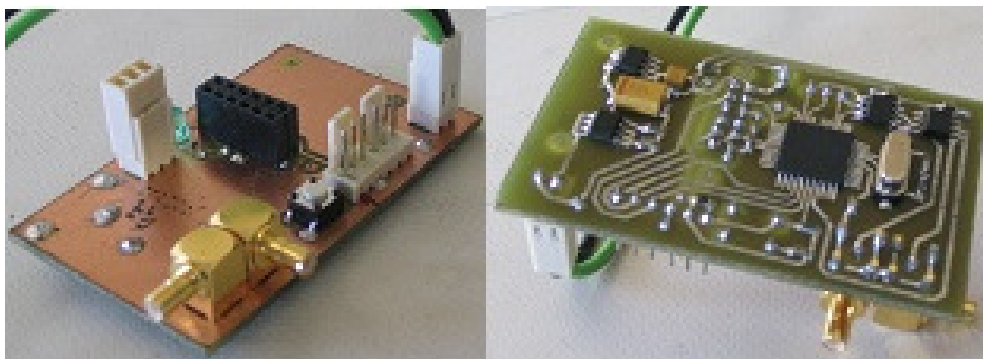


Figure 4.3.1- Control Board photograph

The core of this board consists on a microcontroller, a PIC18LF4520 from Microchip. This microcontroller has several characteristics such as the fact that its supply voltage required range starts on 2.0 V which allows it to be powered by a simple cell phone battery, it has a 10 bit integrated analogue-to-digital converter, low power consumption and incorporates a serial port module to enable data sending to a PC. This microcontroller is also programmable through the serial port and has reduced dimensions with 1cm² of area.

Another important feature of this control board is the possibility of being connected to a wireless module, also available, replacing in a transparent way a serial port without having to change anything in the board. It has a plug that allows the module to be connected or disconnected without having to make any change in the board. The wireless module used is a Bluetooth ParaniESD. The main reason for selecting this module, besides being already available, was its capability of replacing a serial port in a transparent way without having to worry about Bluetooth protocol stack implementation, its supply voltage required being just 3.3V which is important because this way it is possible to power the circuit with a cell phone battery making the system portable and with little weight. Other important features of this module that contributed to the choice made were its small dimensions and its high

range that according to the vendor is of around 100 m allowing the mobility from the patient using the sensor. This module can be seen in 4.3.2.



Figure 4.3.2- Bluetooth module photograph

Besides these important and most visible features of the control board it has another less visible one but as important as the first ones mentioned. For both the microcontroller and the communications module to work perfectly, a constant supply voltage is vital and so a voltage regulator was incorporated in the referred structure. This regulator has a low dropout which means that the voltage difference between its entry and out gates is low. This characteristic is very important because a cell phone battery has a voltage of around 3.7 V and in order to the circuit work without problems it has to have a supply voltage of 3.3 V. Another important characteristic of the voltage regulator is its output current capacity. This is critical because when transmitting data, the Bluetooth module chosen needs a high current capability. The voltage regulator integrated in the control board is a TPS76833Q from Texas Instruments. This regulator needs only 3.5V to be able to supply 3.3V to the circuit so it has a very low dropout as expected. It also has an output current of 1A which is more than sufficient to the designed circuit.

Another feature of the board is a protection circuit against any problems with the battery or from any error with the supply polarity. For this function one has incorporated a simple circuit made with a resistor with a value of some $M\Omega$ and P-channel MOSFET, a Si4425BDY from Vishay. This MOSFET has a low value of r_{DS} which means that when used in a configuration such as the one presented in figure 4.3.3, it behaves like a diode although possessing a smaller voltage drop, between 100mV and 200mV depending on the current that passes through it.

This protection circuit is applied before the voltage regulator, to prevent the destruction of the regulator in case of any problem with the supply voltage.

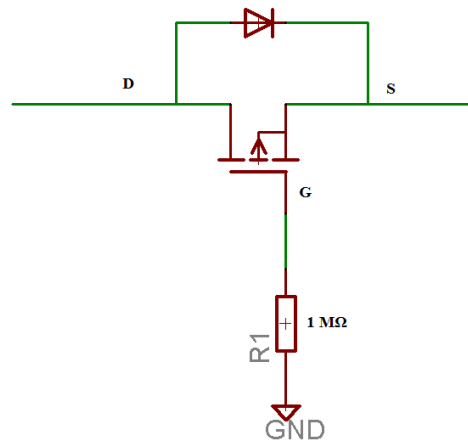


Figure 4.3.3- Protection circuit schematic

A feature not used on this thesis but present in the control board is the LED intensity control. For this function a digital to analogue converter (DAC) was integrated and so it is very simple to control the LED brightness, the only thing need is to send the binary value through the microcontroller serial port then this value is convert to a voltage value that will be imposed to the LED. The DAC chosen was the TLV5623 also from Texas Instruments. This choice was made bearing in mind once more the voltage supply required (only 3.3V), low consumption which is just 1mA and the fact that it possesses an 8-bit interface, compatible with the microcontroller.

As the device will be connected to external elements, such as the bend sensor, it is better to give some kind of protection to those inputs and outputs. For that purpose some operational amplifiers (OPAMPS) on their voltage follower configuration were added. These circuits are rail-to-rail which means that the maximum and minimum values in their outputs are equal to their supply voltages. This is also a critical factor because if the amplifier was limited to a range lower than the difference between the referred values, there would be a limitation on the voltage range used in the ADC and DAC. The model chosen was an OPA2353 from Burr-Brown which includes two amplifiers in its package which is sufficient to this board because it just as one input and one output to protect. This device has a supply voltage requirement compatible with this project since it can be powered with voltages between 2.7 and 5V.

All devices referred above were also selected also in attention to their small size. All of them are in SOIC format measuring only 4x5mm, exception made to the microcontroller. This was a very important characteristic since the purpose is to design a system that can be used by the patient without causing much trouble or discomfort.

Some other components were added to the board and although they do not play a special role, they are essential to the normal operation of the board. In this category the SMB type connectors, with 3mm of diameter specially designed to be used in radiofrequency having very good noise immunity were included. Also in this group there are several decoupling capacitors and a 10MHz crystal to pass to the microcontroller an oscillatory signal to its perfect operation. A reset button and a LED for on/off state indication were also added to the system.

4.4- Graphical Application

The last step in the concept of this smart structure was the creation of a graphical application to better represent data obtained through the sensor. For the development of this tool one has chosen the C programming language and OpenGL graphical library. As for the first choice, the main reasons were the language adaptability and the author's experience in the use of this language. Regarding the graphical library, the election of the OpenGL was due to its relative simplicity in use, its versatility and powerfulness and its capability of incorporation in the language chosen.

This application was planned to have as main functions the data acquisition from a serial port, no matter if it is due to the Bluetooth module or acquired from a test connection through cables, final data processing, data representation in a 3 dimension style and data saving for posterior analysis.

Concerning the first goal, it was necessary to create an external function since it is not possible to access computer hardware directly from a Windows environment. This function uses several other functions present in windows.h library. These functions are CreateFile, ReadFile and CloseHandle. The first one allows the creation of a handle to access and configure a specific hardware such as a serial port while the second one allows the data reading and sending through the same port using the created handle. The third function is essential to prevent errors in port reading. The function created simply opens the serial port, reads data from it and closes it. It returns an integer value representing the digital value obtained by the conversion of the analog voltage value given by the photo-detector.

For the data representation, one needs an angle value and not a voltage value so this is why a final data processing is needed. This conversion is made knowing the relationship between the voltage value read in the photo-detector and the corresponding angle. This relationship is, of course, specific to the sensor created.

After the process described above, the program has a value corresponding to the angle of the bent arm so it is possible to proceed with data representation. It is in this phase that OpenGL is needed. To fulfil this task a simple model of a person was created. This model is based on simpler models such as a sphere and several cubes. These models were created in external files defining their vertices and the normal versors correspondent to each one of the vertices. Positioning these models in the right position allowed the creation of the desired representation of a person. The arm of the figure created is divided into different parts and with the correct rotation of one of the models according to the angle value given by the previous process one can see the arm moving accompanying the movement of the real arm.

Besides this representation, other features are included in this application. In the right upper corner the patient's name is presented and always shown. On the same side of the screen one has to indicate the value of the bending process at a given moment as well as a diagram showing the history of angles achieved while making the test.

Not appearing in the graphical environment but also included in the application deigned is the function of writing in a text file in order to allow a later analysis and evolution of the patient. The application always asks the user to introduce a name so that a file can be created to save these results.

4.5- Concluding Remarks

This chapter presented all the planning made concerning conception of the whole structure with all duly justified choices one had to make.

Regarding the sensor part of the structure, a new method to measure the bending flexion angle was introduced. This procedure is based on the principle of accessing the evanescent field of a side polished POF. As seen in previous work, this field can be related to the bending angle of the fibre since it increases as the bending flexion angle increases. Joining a second side polished POF to the first one in the area treated, one can couple this evanescent field to the added fibre being able to measure its value and, therefore, being able to estimate an angle.

With respect to the control board, this electronic circuit is responsible for data acquisition (receiving the signal from the sensor created), data processing (convert data to a digital format) and data sending. This last function is made by a Bluetooth module to enable wireless data sending which gives this whole structure true portability.

On the topic of the graphical application, the choice of C language and the graphical library OpenGL was made due to their adaptability and simplicity as well as the author's experience with both tools.

5. Results

5.1- Introduction

In this chapter the most important results obtained throughout the implementation of this thesis are exhibited as well as the experience conceived to obtain those same results.

5.2- Sensor

The first thing to do is to ascertain whether it is possible to do the operation of bend sensing with a simple POF. For this and all other experiments, an arm simulator made of wood was built in order to imitate how the sensor would behave in a real arm environment. Another constant in all experiments is the POF used. This fibre is from the HFBR-R/EXXYYYZ series with diameter of 2.2mm including jacket. This choice was made as a result of several advantages of this type of fibres such as easy non-skilled handling, ruggedness, low cost, large diameter and mechanical resistance. For these tests, the amplifier described on chapter 4 was not used because this circuit is only necessary to achieve better resolution in the conversion using the ADC of the microcontroller, dispensable at this stage of the test. The arm simulator and the results obtained in this first experiment can be seen in figure 5.2.1 and figure 5.2.2, respectively. During the measurements done in this thesis consider that the bending flexion angle is the smaller angle between the arm and the forearm.



Figure 5.2.1- Arm simulator photograph

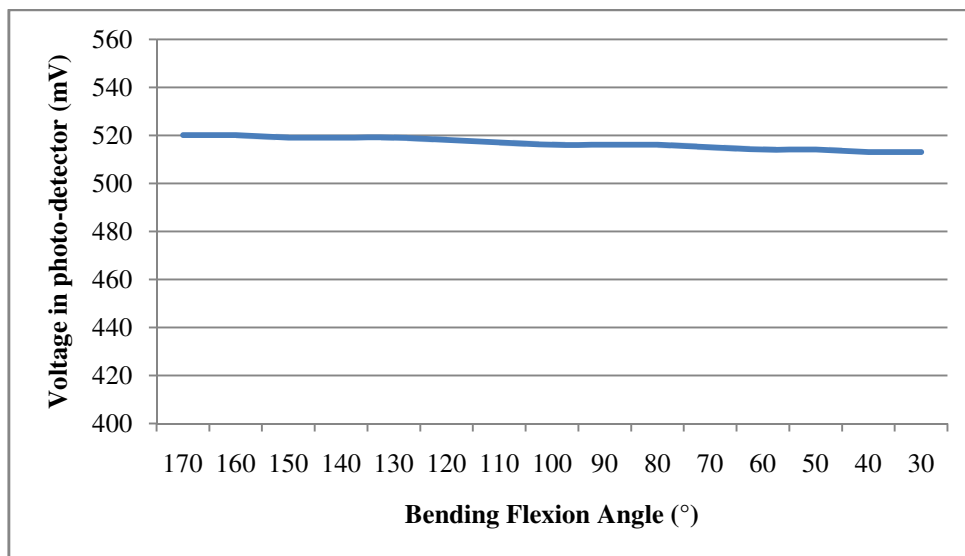


Figure 5.2.2- Voltage vs Angle with a single POF

As shown in figure 5.2.2, the simple POF is not good when used as a bend sensor. As expected, the bend losses are very low which would result in a low sensibility to any angle variation. This procedure was therefore abandoned and other alternatives were sought.

The alternatives found were based on creating imperfection on the fibre in order to increase losses during the bending process and, therefore, creating a good sensibility to angle changes. As shown on chapter 3 there are several alternatives to perform a bend sensing. However, only some of them were tested due to the complexity of doing a LPG in a polymer optical fibre and due to the inexistence of a solvent capable of creating a taper in the available POFs. Using the arm simulator shown on figure 5.2.1 some measures were made and the results obtained with some of the presented techniques are shown on figure 5.2.3.

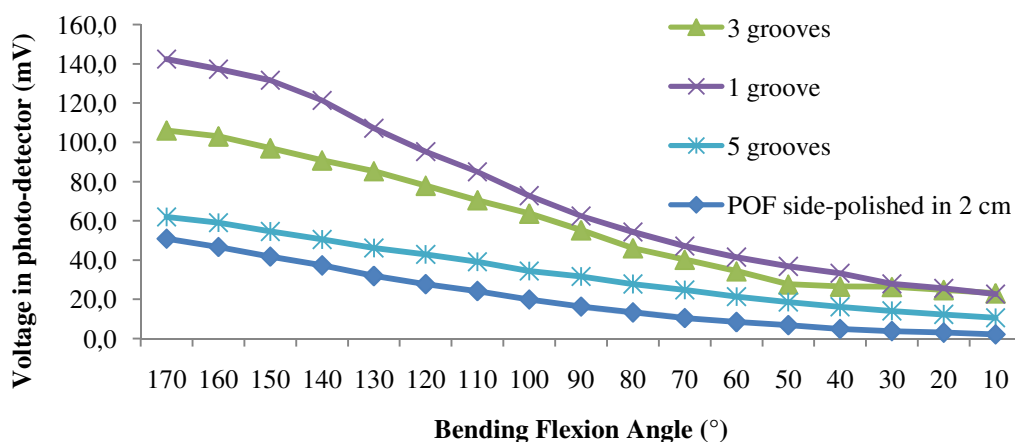


Figure 5.2.3- Results obtained with different techniques of increasing sensibility in POF

As for the technique of creating grooves in the fibre, different numbers of imperfections were experimented. All grooves were created with depth of 50% of the original diameter of the POF. One notices that this technique really increases bend sensibility but as the number of grooves increase this sensibility decreases. This is due to the growing of losses caused by the imperfections, therefore the best results were obtained with just one groove. Regarding the side polished POF, the imperfection was created also with depth of 50% of the original diameter of the fibre and length of 2 cm. Despite having a smaller initial voltage at the angle of 180°, it also enhances a good sensibility since it returns a very low voltage at 0° angle.

As stated before a new method of bend sensing was proposed. This method is based on a variable coupler made of two side-polished POFs and its operation was explained on chapter 4. In order to ascertain the viability of this procedure, several tests were made. Three couplers were built with different lengths of polished surface. All three couplers were polished with a depth of 50% of the POF initial diameter. This polishing was made with a handling polishing machine, a Logitech PM2. Results obtained in this experiment are displayed in figure 5.2.4.

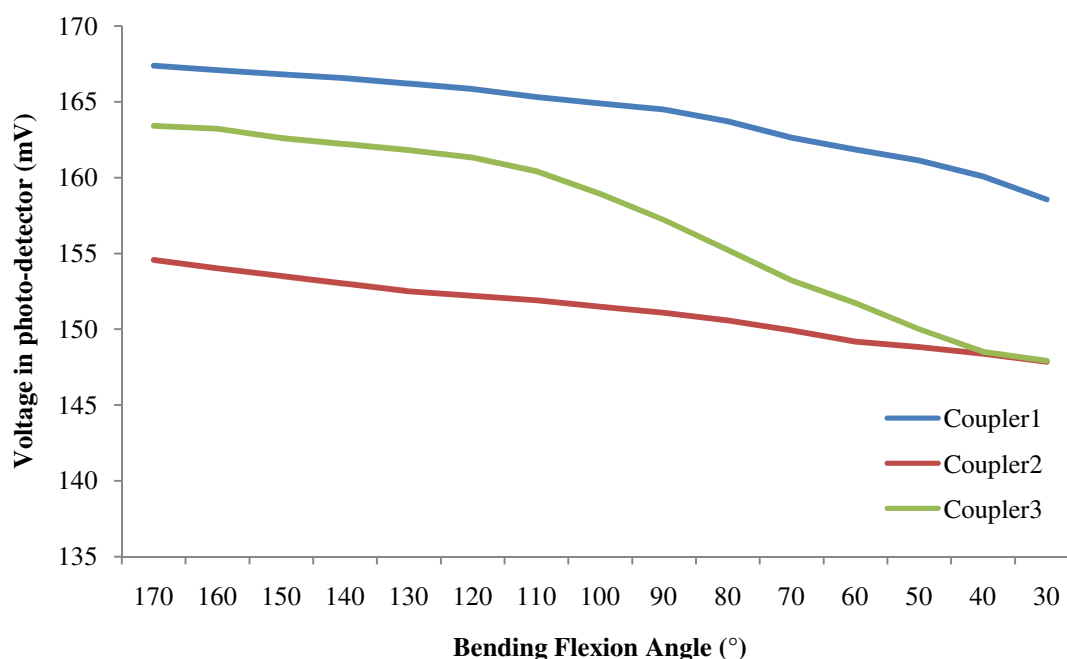


Figure 5.2.4- Power attenuation due to bending angle on three different couplers (coupler1 with 1.4 cm of polished area length; coupler 2 with 1.0 cm of polished area length; coupler 3 with 2.0 cm of polished area length)

As for coupler 1 and coupler 2 one can notice that their response to bending is similar despite having a recurrent difference of voltage between them. This difference is due to the

discrepancy of polishing lengths. When this measure is smaller the coupling is worse and therefore the voltage value read in the photo-detector is also smaller. This indicates that a pattern of behaviour was achieved and, as expected, there is a real dependence between coupling and the polished length. Concerning the third coupler, it was found an unusual behaviour when compared to the other sensors. Despite having a larger polished area which should indicate a better coupling, this value was worse than the sensor with length of 1.4 cm. Another difference was the variation obtained through all angle range. While the first two couplers had a variation of, approximately, 10 mV in the voltage read between 30° and 180°, the third one had a variation of 20 mV which means twice the sensibility. This behaviour was probably due to errors in fabrication since this process is done manually without having the precision required. On the process of fabrication of these sensors, the only thing one has the possibility to control is the time of the process itself and not the pressure that is applied to the fibre. Despite having used the same time values for all three couplers, a variation of depth polished may exist which can explain the variation of behaviours observed. Regardless of the results, the sensor used was the third one. This choice was made because this coupler had the best reaction to the purpose of this thesis as it had a better sensibility to bending than the other two specimens.

When the sensor was fully operational, it was necessary to build a PCB for hosting both the LED and the photo-detector. This PCB should be as small as possible in order to cause as little discomfort in the patient's arm. It was decided to build just one PCB for the light emitter, receiver and amplifier in order to diminish the number of cables used and taking advantages of low bending losses of a POF. A photograph of the built board is shown on figure 5.2.5.

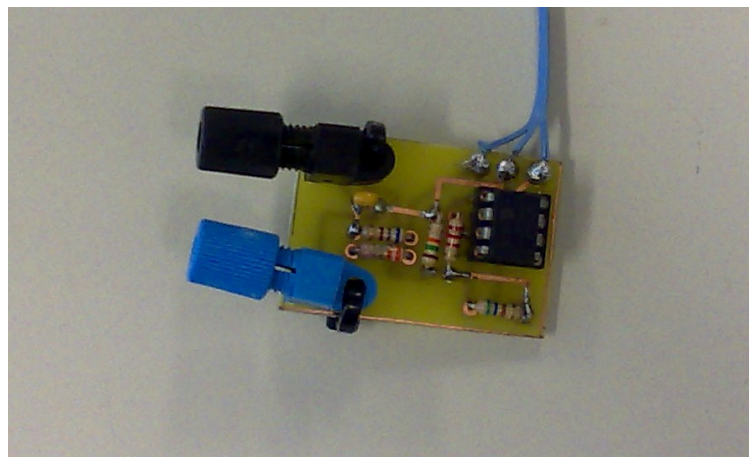


Figure 5.2.5- Light emitter, receiver and amplification circuit photograph

After having the shown PCB ready and functional, the next step was to apply firmly both the sensor and the referred board to a sleeve that should be close fitting. This tightness of

the sleeve is essential in order to allow the sensor to follow the arm during the bending process. To ensure that the fibre suffered the flexion only in the intended area two hollow tubes made of a rigid material were glued to the sleeve. When placing the sensor in an arm, one must pay attention to the position of the area between both tubes because this area must be placed right in the elbow joint on the outside side of the arm. A photograph of the sensor placed on the sleeve as well as another showing the same structure correctly placed in the arm are shown in figures 5.2.6 and 5.2.7 respectively.



Figure 5.2.6- Photograph of the sensor applied on the sleeve



Figure 5.2.7- Photograph of the sensor correctly applied in the arm

With the sensor placed in the position exhibited above several measures were taken to observe the behaviour of the coupler applied in the arm. These measures are shown in figure 5.2.8.

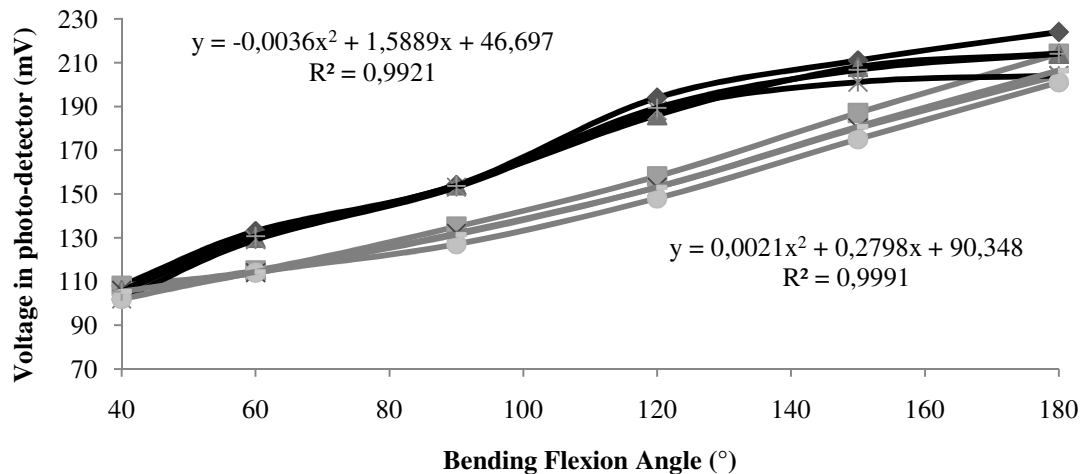


Figure 5.2.8- Voltage vs bending flexion angle with the sensor applied in a real arm (3 cycles bending/extension with black lines representing bending process and grey lines showing extension process)

Observing the graphic, one can see that measurements of the sensor, behave in two different ways due to hysteresis. When bending the arm, values are always higher than when doing the opposite movement. As one can see in the same graphic, although during the bending or extension process, the sensor behaves in the same way generating voltage values very similar to each other, these values have been acquired using the amplification circuit with gain of 4. So the real difference is 4 times smaller than the graphic shows. Another detail one has to pay attention to is the fact that one took measures of certain angles due to the difficulty of achieving higher accuracy when placing the elbow joint with a certain angle. For that reason, only 180°, 150°, 120°, 90°, 60° and 40° angles were considered.

5.3- Control Board

At this stage, one already has an analogue signal from the sensor ready to be processed by the microcontroller. From this point on all attention will be focused on the control board and on the process of obtaining the signal by the PIC, transforming it to a format ready to be sent and on the actual action of sending it to the computer.

The first test needed was to ascertain if the control board is totally functional and if it is possible to send any information to the computer. In order to do this, and for test use only, a simple circuit was built to direct data through a serial port. This simple circuit is composed by a MAX232 and several capacitors. The only function of this structure is to convert a signal from TTL voltages (0 and 5V) to voltages acceptable to be sent through a normal cable serial port (± 12 V). This is only needed at testing stage because after that the Bluetooth module will handle this procedure. The circuit referred can be seen in figure 5.3.1.

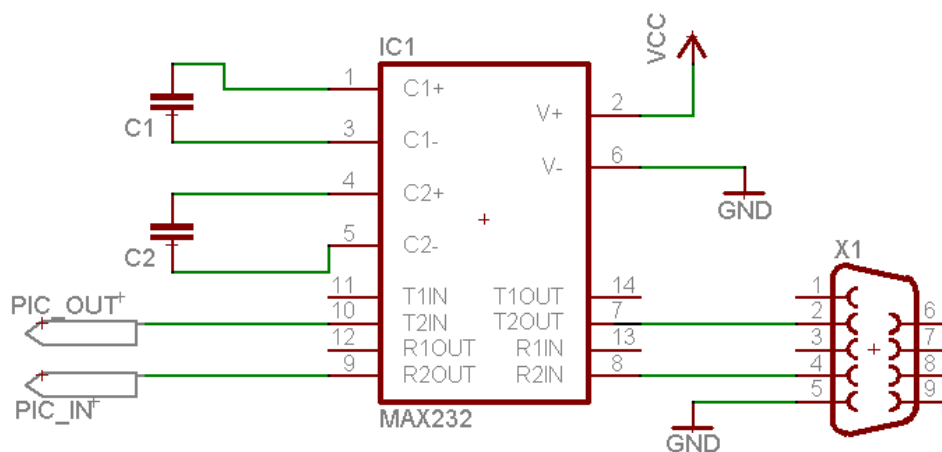


Figure 5.3.1- MAX232 circuit schematic

To check if the control board was functional, it was powered with the correct polarity and, with the circuit described above connected to the control board. The PIC was programmed for the first time with a simple program that tried to write in the computer the string "555!". The program editing and compilation was made using SourceBoost IDE, an editor with a freeware C compiler and a linker included. After developing this simple program, it was sent to the microcontroller with WinPIC Loader and this process took place with no problems. In order to see the information in the computer one needed a terminal program that could read its serial port. For this purpose, the chosen program was HyperTerminal,

simple to use and a free program that is already included in Windows. In this software and after doing the initial configuration the expected results were achieved. These results are shown on figure 5.3.2.

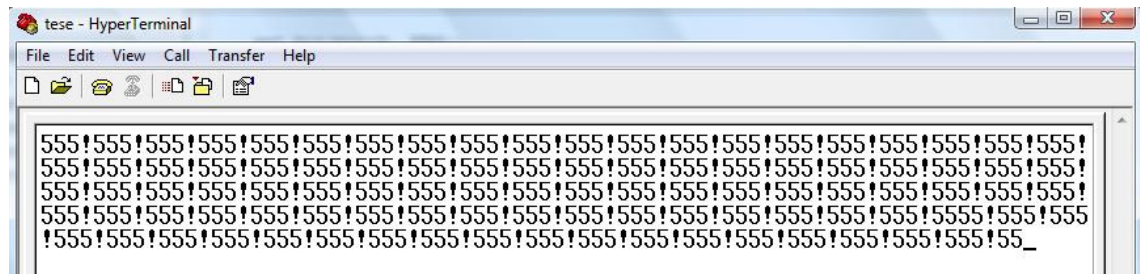


Figure 5.3.2- Hyperterminal showing values sent by the PIC

After achieving these results one came to the conclusion that the control board was functional and that one could proceed on to the next test.

The following step was to adapt the program written in the microcontroller to read and send a value from its ADC instead of sending a fixed value or string chosen by the programmer. For this purpose, modifications and configurations were made accordingly. After this procedure the results obtained were the ones shown in figure 5.3.3. The values shown are directly resulting from the ADC conversion and therefore are in a range from 0 to 1024 where 0 represents 0V and 1024 represents 3.3V.

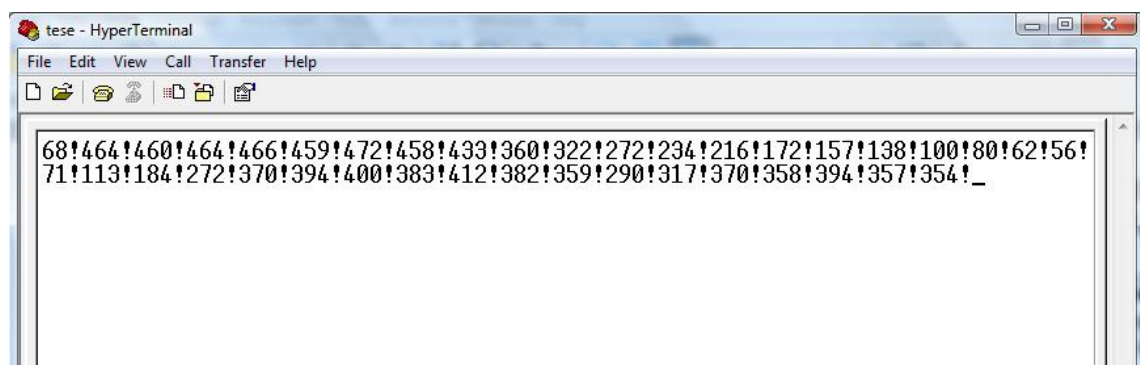


Figure 5.3.3- Hyperterminal showing the direct result of the ADC conversion

The last step of this series of tests was to experiment if the system behaviour was constant whether the communication was made through a serial port or through the Bluetooth module. For that purpose the module was plugged into the board and the program written

in the microcontroller was changed again in order to perform the reset of the referred module needed to do its correct initialization. This pin must be in 0V status for, at least, one second according to the Bluetooth datasheet. After this process the module is fully functional and ready for pc synchronization. For this purpose another external software is needed to proper connect the module to the pc. The chosen software was BlueSoleil from IVT Corporation. Next to this step, the Bluetooth module is ready to function as a serial port and all applications needing data from the control board just have to configure a serial port with the same parameters programmed in the Bluetooth module which are, for default, 9600bps, 8 data bits, none flow control and 1 stop bit.

5.4- Graphical Application

The graphical application designed has the purpose of giving a better display of what is happening to the arm and allow data saving for future analysis. For this purpose, the referred application was created with the OpenGL graphics library to give a 3D image of the situation. This program initially asks to the user what are the patient's name and the name of the file to be created in order to save results. After this initial step, the program opens three different windows showing an environment like the one shown in figure 5.4.2. On the left window, a simple representation of a human body was drawn in which the arm moves accordingly to the patient's movement. In the window on the top right corner of the figure are shown the patient's name as well as the current angle value of the arm. Finally, are shown in the window on the bottom right corner, a 2D plot was designed to show the behaviour of the arm since the beginning of the test.

As to the other function of the graphical application, the creation of a file to allow further analysis, this was also achieved. In this text file is varied information on the test, such as the patient's name, the date and time that the test began and the values obtained with the corresponding time that they were reached, is saved. The next figure shows an example of a text file created.

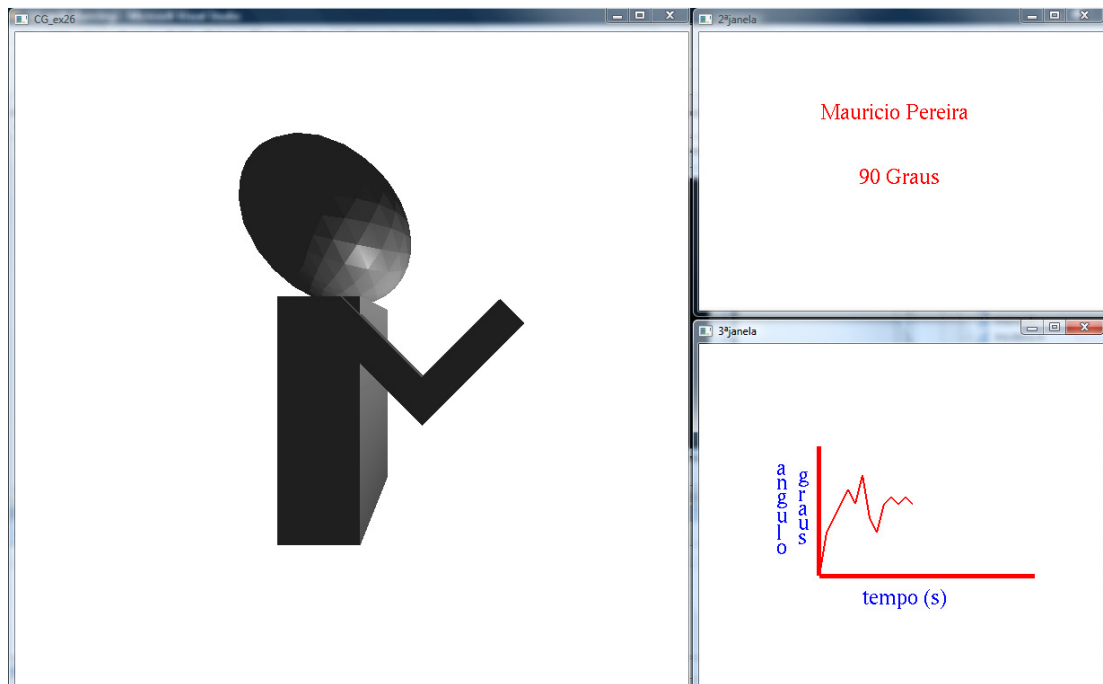


Figure 5.4.1- Graphical Application environment

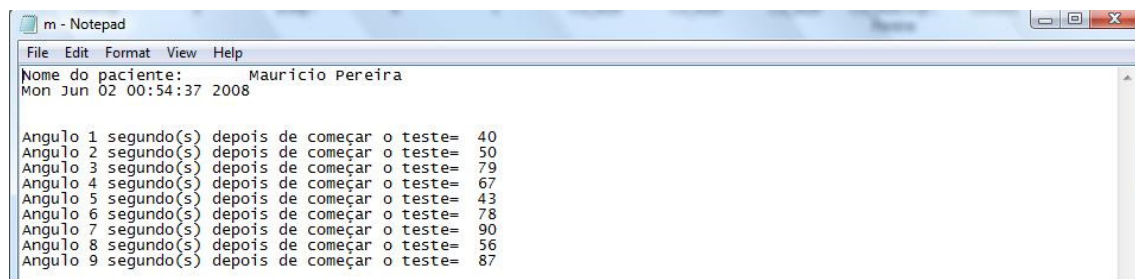


Figure 5.4.2- Output text file of the graphical application

5.5- Concluding Remarks

With the aim of somehow innovate on the bending sensors technology, a new method to perform bend sensing was introduced. In this chapter, the performance of the approach now conceived was compared to other well known procedures and the dependence of performance of this new technique with the length of polished fibre is demonstrated.

As for the dependency of sensibility on the polished length, one can notice that despite the coupling effect being better as one increase the treated area, the responsiveness to bending does not increase. As for the comparison with the other methods, it can be noticed that despite not having such responsiveness as creating other type of imperfections on the fibre, this is a possible and valid way to perform this kind of measurement.

The results show that the sensor created suffers from hysteresis which was already expected since performing bend sensing using just a side polished fibre is already affected by this effect. Despite producing a not ideal behaviour, this effect by itself does not jeopardize the intended aim because what matters is that the coupler has always the same response to the same movement, which it has. The fact of having two different responses to opposite movements can be easily solved by programming two different functions in the graphical interface to detect if it is a bending or an extension movement that is taking place.

One problem observed in this method is the recovery time of the sensor. As the sensor is made of plastic polymers it takes a little time to regain its original position when severely bended. This inconvenient is increased by the use of duct tape to unite the coupler. This can be a problem when using this sensor to continuously monitor the flexion of a patient's arm although it is not a very important factor when being used in a rehabilitation test.

In order to achieve good results with this sensor, one has to be very careful when positioning the sensor in the arm. The free zone of the sensor must be placed right over the joint of the elbow in the outer side of the arm. Obviously, to get consistent results, the sensor must be placed always in the same side of the arm and in the same position.

Regarding the electronic part of this wearable sensor, the control board revealed itself with capable enough to perform correctly the function that it was designed for and has the advantages of being small, lightweight and able to be powered with just a cell phone battery enabling its use with low discomfort to the patient. One limitation of this board is the memory capacity. The capacity of storing values is limited to the PIC memory, which is approximately around 32Kbytes for both data and program, which means that one can store measurements made during a little more than 4 hours with a second of interval between each data collection. This restriction does not leave much margin to create different modes of operation, for example, by disabling the value sending when performing a continuous test during a whole day without the user being near to a pc.

Concerning the graphical application element it was designed a simple but illustrative one to show the instant reality as well as the recent behaviour of the patient's arm.

6. Conclusions

With the realization of this thesis it was once more demonstrated that optical fibres are suitable for use as sensors, more precisely, bend sensors. Despite requiring a responsiveness enhancement, optical fibres have a monotonous response to bending which allows its accurate measurement and together with their light weight, low cost (polymer optical fibres) and electromagnetic immunity characteristics make fibres excellent sensors especially for portable applications.

There are several methods to enhance fibre sensitivity to the bending process but all approaches are based on the creation of imperfections in the fibre to increase light losses when the referred action is occurring. As these losses are dependent on the amount of flexion the fibre is suffering, a relationship between both facts can be found and therefore bend sensing can be performed. Another procedure based on the same principle was presented in this thesis. The technique proposes the variable coupler that has the coupling ration dependent on the bending flexion angle. With this technique a variation of around 30 mV in the voltage measured for a 130 degrees angle range. Despite the fact the sensor created suffer from hysteresis, it has a constant and monotonous behavioural response and therefore this problem can be easily surpassed by programming two different functions to distinguish a flexion movement from a extension movement.

A smart structure using the created sensor was also designed in order to perform data treatment and enable the possibility of its use wirelessly and always having the purpose of causing as small discomfort to the person being tested as possible.

7. Future Work

Despite having created a new method to perform bend sensing in a portable device comfortable to the patient and capable of achieving good results, there are more features one can add to improve the designed structure.

One aspect that can be explored is the comparison of optical methods of bend sensing with other electronic methods such as accelerometers. These can also be combined with optical methods in order to measure not only bending but also rotation and the movement acceleration.

The possibility of using a cascaded group of this type of sensors in order to measure the same bending process in several different angles to achieve more accurate results can be studied. The same procedure can be used to perform the same measurements in different human joints, for example, the elbow and shoulder.

In the electronic part, a memory block can be added to improve the memory capability of the control board. This can be useful to perform continuous tests without the necessity of being near a computer. Data could be saved in the local memory and, only after the test, could then be transferred to the computer for data representation.

Regarding the last part of the designed concept, the graphical application, this could be written in other programming language, such as Java or C#, in order to enable the possibility of using this application in a PDA or in a regular cell phone since they are capable of communicating with the control board by Bluetooth technology.

8. References

- [1] A Appajaiiah, Climatic Stability of Polymer Optical Fibres (POF), 2004
- [2] Daum, Krauser, Zamzow and O Ziemann, Polymer Optical Fibres for Data Communication, Springer 2005.
- [3] Abe T, Mitsunaga Y and Koga H, Strain sensor using twisted optical fibres, Opt. Lett. 9 373, 1984
- [4] Berthold J W, Historical review of microbend fibre optic sensors, J. Lightwave Technol. 13 1193, 1995
- [5] Stephen W J and Ralph P Tatam, 2003 Optical fibre long-period grating sensors: characteristics and applications, Meas. Sci. Technol. 14 (2003) R49–R61
- [6] H.J. Patrick, C.C. Chang and S.T. Vohra, Long period fibre gratings for structural bend sensing, ELECTRONICS LETTERS 3rd September 1998 Vol. 34 No. 18
- [7] D.F. Merchant, P.J. Scully and N.F. Schmitt, Chemical tapering of polymer optical fibre, Sensors and Actuators 76 1999 365–371
- [8] R Philip-Chandy, P J Scully and R Morgan, The design, development and performance characteristics of a fibre optic drag-force flow sensor, Meas. Sci. Technol. 11 (2000) N31–N35
- [9] A Babchenko and J Maryles, A sensing element based on 3D imperfedted polymer optical fibre, J. Opt. A: Pure Appl. Opt. 9 (2007) 1–5
- [10] K S C Kuang, W J Cantwell and P J Scully, An evaluation of a novel plastic optical fibre sensor for axial strain and bend measurements, Meas.Sci.Technol. 13 (2002) 1523–1534
- [11] A Babchenko, Z Weinberger, N Itzkovich and J Maryles, Plastic optical fibre with structural imperfections as a displacement sensor, Meas. Sci. Technol. 17 (2006) 1157–1161
- [12] L E Dunne, P Walsh, B Smyth and B Caulfield, Design and Evaluation of a Wearable Optical Sensor for Monitoring Seated Spinal Posture, Proceedings of IEEE International Symposium on Wearable Computers; 65-68; October 2006;
- [13] Lomer, M.; Quintela, A.; López-Amo, M.; Zubia, J.; López-Higuera, J. M., A Quasi-distributed Level Sensor Based on a Bent Side-Polished Plastic Optical Fibre Cable, Measurement Science and Technology; 18; 2261-2267; 2007-09-13;
- [14] L Bilro, R Nogueira and J L Pinto, Flexion angle measurements with an optical fibre goniometer, PTEE 2007
- [15] <http://www.cem2.univ-montp2.fr/~moreau/jBPM/index.html>